Manuscript Details

Manuscript number	BBR_2018_1571_R1
Title	Plasticity of paternity: effects of fatherhood on synaptic, intrinsic and morphological characteristics of neurons in the medial preoptic area of male California mice
Article type	Research Paper

Abstract

Parental care by fathers enhances offspring survival and development in numerous species. In the biparental California mouse, Peromyscus californicus, behavioral plasticity is seen during the transition into fatherhood: adult virgin males often exhibit aggressive or indifferent responses to pups, whereas fathers engage in extensive paternal care. In this species and other biparental mammals, the onset of paternal behavior is associated with increased neural responsiveness to pups in specific brain regions, including the medial preoptic area of the hypothalamus (MPOA), a region strongly implicated in both maternal and paternal behavior. To assess possible changes in neural circuit properties underlying this increased excitability, we evaluated synaptic, intrinsic, and morphological properties of MPOA neurons in adult male California mice that were either virgins or first-time fathers. We used standard whole-cell recordings in a novel in vitro slice preparation. Excitatory and inhibitory post-synaptic currents from MPOA neurons were recorded in response to local electrical stimulation, and input/output curves were constructed for each. Responses to trains of stimuli were also examined. We quantified intrinsic excitability by measuring voltage changes in response to square-pulse injections of both depolarizing and hyperpolarizing current. Biocytin was injected into neurons during recording, and their morphology was analyzed. Most parameters did not differ significantly between virgins and fathers. However, we document a decrease in synaptic inhibition in fathers. These findings suggest that the onset of paternal behavior in California mouse fathers may be associated with limited electrophysiological plasticity within the MPOA.

Keywords	electrophysiology; hypothalamus; medial preoptic area; neuronal morphology; parental care; paternal care

Corresponding Author	Wendy Saltzman
Corresponding Author's Institution	University of California, Riverside
Order of Authors	Nathan Horrell, Wendy Saltzman, peter hickmott

Suggested reviewers	Brian Trainor, Michael Numan, Roland Johansson

Submission Files Included in this PDF

File Name [File Type]

Response_to_Reviewers_BBR_2018_1571-R1_Horrell.pdf [Response to Reviewers]

Highlights_BBR_2018_1571-R1_Horrell.pdf [Highlights]

Manuscript_BBR_2018_1571-R1_Horrell.pdf [Manuscript File]

Fig1_BBR_2018_1571-R1_Horrell.pdf [Figure]

Fig2_BBR_2018_1571-R1_Horrell.pptx [Figure]

Fig3_BBR_2018_1571-R1_Horrell.pptx [Figure]

Fig4_BBR_2018_1571-R1_Horrell.pptx [Figure]

Fig5_BBR_2018_1571-R1_Horrell.pptx [Figure]

Fig6_BBR_2018_1571-R1_Horrell.pptx [Figure]

Fig7_BBR_2018_1571-R1_Horrell.pptx [Figure]

Fig8_BBR_2018_1571-R1_Horrell.pptx [Figure]

Table1_BBR_2018_1571-R1_Horrell.pdf [Table]

Table2_BBR_2018_1571-R1_Horrell.pdf [Table]

Table3_BBR_2018_1571-R1_Horrell.pdf [Table]

Table4_BBR_2018_1571-R1_Horrell.pdf [Table]

Table5_BBR_2018_1571-R1_Horrell.pdf [Table]

Table6_BBR_2018_1571-R1_Horrell.pdf [Table]

Table7_BBR_2018_1571-R1_Horrell.pdf [Table]

Table8_BBR_2018_1571-R1_Horrell.pdf [Table]

Table9_BBR_2018_1571-R1_Horrell.pdf [Table]

Table10_BBR_2018_1571-R1_Horrell.pdf [Table]

SupplementalTable1_BBR_2018_1571-R1_Horrell.pdf [Table]

To view all the submission files, including those not included in the PDF, click on the manuscript title on your EVISE Homepage, then click 'Download zip file'.

Wendy Saltzman
Evolution, Ecology, and Organismal Biology
University of California, Riverside
Riverside, California 92521 USA
Voice: (951) 827-6356
FAX: (951) 827-4286
E-mail: Saltzman@ucr.edu

February 15, 2019

Dear Drs. Huston and Maren,

Attached please find a revision of our manuscript, "Plasticity of paternity: effects of fatherhood on synaptic, intrinsic and morphological characteristics of neurons in the medial preoptic area of male California mice." We are very grateful to the reviewers for their thoughtful and constructive comments on the previous submission of the manuscript. Our responses are as follows:

Reviewer 1

"The authors found that MPOA neurons in fathers showed lower maximal evoked IPSCs than virgins, indicative of a decrease in MPOA inhibition in fathers. The authors need to interpret this finding in more detail and discuss its relevance. Does this major finding mean that the effects of natural inhibitory inputs to MPOA would be dampened in fathers? Where might such neural afferents to MPOA come from? What might be the underlying mechanisms within MPOA neurons that cause this dampened inhibitory response? Since the output of MPOA is so important for parental behavior, answers to these questions are crucial and should be enlightening."

We agree that an expounding on the possible mechanisms of a decrease in maximal IPSCs in fathers is needed and have added several sentences about this in the discussion (lines 322-340). These are important questions, and answering them experimentally may reveal components of plasticity facilitating paternal behavior in California mice.

"As an example, it has been suggested in rats that PAG input to MPOA might depress parental behavior. It would have been interesting to explore whether natural afferent inhibitory inputs to MPOA neurons are depressed in fathers."

Yes, investigating specific MPOA afferents or efferents implicated in parental care would have been valuable. Unfortunately, this is beyond our capabilities currently. We now mention this point in the last paragraph of the discussion (lines 383-385).

"I think there may be an error in Figure 5B, although it is possible that I am not reading it correctly. When comparing Figure 5B with the data in Table 9, it appears that the data in Figure 5B is reversed. This figure shows that fathers, rather that virgins, have higher IPSC amplitudes, while the reverse it what is reported in the text and in Table 9. If I am interpreting Fig. 5B incorrectly, the authors should modify the text to aid the reader in interpreting the figure properly."

Thank you for pointing this out. Yes, the colors in Fig. 5 were inadvertently switched. This has now been corrected.

Reviewer 2

Wendy Saltzman
Evolution, Ecology, and Organismal Biology
University of California, Riverside
Riverside, California 92521 USA
Voice: (951) 827-6356
FAX: (951) 827-4286
E-mail: Saltzman@ucr.edu

Comments about correlations:

> "Thus, looking at correlations within virgin males with behavior could provide additional clues to MPOA function. Even if this approach did not pan out, this will still be an important paper because so little is known about the electrophysiological properties of MPOA neurons."
>
> "It might be interesting to look at correlations within virgin males to see if individual variation in parental care was associated the different electrophysiological parameters."
>
> "As with the other ephys variables, did the authors look at correlations between neuronal morphology metrics and paternal behavior, especially as this was the primary approach used in the Parent et al. 2017 study."

Thank you for this suggestion. We have now performed correlational analyses between key behavioral measures (i.e., latency to initiate paternal care, percent time spent in paternal behavior) and many electrophysiological and morphological variables. These correlations add a new dimension to the paper, although after correcting for false discovery rate, no significant correlations were found. The methods (lines 218-224) and results (lines 282-292) now include information about these correlations, and a new table has been added (Supplemental Table 1).

"The authors state that little is known about the electrophysiological properties of MPOA neurons. It seems like it would be relevant to give a short overview of what is known and whether the authors expected to see different results in this study."

A brief review of the known electrophysiological properties of MPOA neurons occurs in the discussion (lines 344-352). We have added additional information and state our expectations that targeting specific cell types, such as cells that express estrogen receptors or the neuropeptide galanin, for reasons explained in the discussion, may reveal differences.

"Were mice randomly assigned to be paired with a female?"

Mice were assigned into categories of "virgin" or "father" in an aged-matched but otherwise random fashion throughout the experiment. We now mention this in the methods (lines 104-106).

"On line 241 it would be easier to compare the different parameter by grouping together the properties and listing virgins and fathers next to each other."

Thank you for this suggestion. We have re-written this sentence accordingly (lines 248-249).

"Also, did the authors try using a chi-square test to see whether these percentages really were similar in fathers and virgins? For example there were almost 42% regular spiking neurons in fathers and vs 29% in virgins."

Wendy Saltzman
Evolution, Ecology, and Organismal Biology
University of California, Riverside
Riverside, California 92521 USA
Voice: (951) 827-6356
FAX: (951) 827-4286
E-mail: Saltzman@ucr.edu

Because our data did not meet the requirements for a chi-square test (i.e., expected values of some cells were <5), we conducted Fisher's exact tests and Freeman-Halton extension of Fisher's exact tests (lines 250 & 270). We found no differences in percentages of neurons in certain categories in virgins and fathers.

"Line 270, the authors should state how many individual mice were examined in addition to number of cells."

The numbers of mice and cells are now stated (line 277).

"I think the authors should address differences in IPSCs earlier in the discussion and make more of an effort to discuss the potential behavioral significance. Based on the literature, what would a decrease in IPSCs do to MPOA function? What is the main source of inhibitory input into the MPOA? How would an increase in IPSC's be expected to alter MPOA function. The authors might be able to draw more from the sexual behavior literature to develop these lines of thought."

Several sentences, some of which comprise a new paragraph, have been added to the discussion to address the plausible mechanisms of decreased inhibition in the MPOA and sources of inhibitory input into the MPOA (lines 328-347). Due to the nature of our preparation, complex connectivity, and heterogeneity of cell types in the MPOA, we do not want to speculate too much on what precisely is going on, though answering these questions in future experiments using methods now mentioned in the discussion is a goal.

"The discussion on biochemical mechanisms of paternal behavior is thoughtful. Perhaps an avenue for future research is to test whether estradiol (or other hormones) has different effects on neurophysiological parameters in fathers vs virgins?"

Thank you for this suggestion. We agree that the possibility of hormonal effects being dependent on reproductive status (e.g., virgin or father) is intriguing and could be an interesting topic for future studies. We now mention this in the discussion as a possible future direction (lines 365-366).

Thank you for your consideration. We look forward to hearing back from you.

Yours sincerely,

Wendy Saltzman

Wendy Saltzman
Professor, Department of Evolution, Ecology, and Organismal Biology

Highlights

- California mouse fathers provide extensive paternal care to their offspring.
- We compared properties of medial preoptic area neurons of fathers and virgin males.
- Few differences were seen in intrinsic, synaptic, or morphological properties.
- Synaptic inhibition was lower in fathers than in virgin males.
- Fathers exhibited more paternal behavior toward unfamiliar pups than virgin males.

Plasticity of paternity: effects of fatherhood on synaptic, intrinsic and morphological characteristics of neurons in the medial preoptic area of male California mice

Abbreviated title

Plasticity of paternity in medial preoptic area

Authors

Nathan D. Horrell[1,2], Wendy Saltzman[1,2], and Peter W. Hickmott[1,3]

Affiliations

[1]Graduate Program in Neuroscience, [2]Department of Evolution, Ecology, and Organismal Biology, [3]Department of Psychology, University of California, Riverside, CA 92521

Corresponding Author

Wendy Saltzman

Department of Evolution, Ecology, and Organismal Biology

University of California, Riverside

900 University Ave.

Riverside, CA 92521

e-mail: saltzman@ucr.edu

Conflict of Interest

The authors declare no competing financial interests.

Abstract

Parental care by fathers enhances offspring survival and development in numerous species. In the biparental California mouse, *Peromyscus californicus*, behavioral plasticity is seen during the transition into fatherhood: adult virgin males often exhibit aggressive or indifferent responses to pups, whereas fathers engage in extensive paternal care. In this species and other biparental mammals, the onset of paternal behavior is associated with increased neural responsiveness to pups in specific brain regions, including the medial preoptic area of the hypothalamus (MPOA), a region strongly implicated in both maternal and paternal behavior. To assess possible changes in neural circuit properties underlying this increased excitability, we evaluated synaptic, intrinsic, and morphological properties of MPOA neurons in adult male California mice that were either virgins or first-time fathers. We used standard whole-cell recordings in a novel *in vitro* slice preparation. Excitatory and inhibitory post-synaptic currents from MPOA neurons were recorded in response to local electrical stimulation, and input/output curves were constructed for each. Responses to trains of stimuli were also examined. We quantified intrinsic excitability by measuring voltage changes in response to square-pulse injections of both depolarizing and hyperpolarizing current. Biocytin was injected into neurons during recording, and their morphology was analyzed. Most parameters did not differ significantly between virgins and fathers. However, we document a decrease in synaptic inhibition in fathers. These findings suggest that the onset of paternal behavior in California mouse fathers may be associated with limited electrophysiological plasticity within the MPOA.

Keywords

electrophysiology, hypothalamus, medial preoptic area, neuronal morphology, parental behavior

1. Introduction

Parental care by mothers occurs in all mammalian species, while care by fathers occurs in only approximately 5-10% of mammals. Infant-directed behavior of males in biparental species can range from infanticide to avoidance to paternal care, and a male can display all three behaviors in his lifetime (Kleiman & Malcom, 1981; Woodroffe & Vincent, 1994).

The monogamous California mouse (*Peromyscus californicus*) exhibits a biparental care system, in which both parents provide extensive care to their offspring (Ribble & Salvioni, 1990; Ribble, 1991; Gubernick & Teferi, 2000). Fathers perform the same parental behaviors (except nursing) as mothers, and to a similar extent (Dudley, 1974; Gubernick & Alberts, 1987). Male California mice typically exhibit a shift in pup-directed behavior during the transition into parenthood: virgin males often exhibit infanticide or indifference when exposed to unrelated pups, whereas fathers exhibit paternal care (de Jong et al., 2009; Gubernick & Alberts, 1987). Thus, the California mouse is a useful model for investigating neural and hormonal plasticity underlying the onset of paternal care.

The neurobiological substrates of parental behavior have been examined much more extensively in females than in males. One of the brain regions most strongly implicated in maternal behavior is the medial preoptic area (MPOA) of the hypothalamus (see reviews by Numan & Insel, 2003; Numan, 2006, 2014; Dobolyi, Grattan & Stolzenberg, 2014). In rats (*Rattus norvegicus*) and house mice (*Mus spp*.), c-fos is elevated in the MPOA after females are exposed to pups and/or engage in maternal care (Komisaruk et al., 2000; Lonstein & De Vries, 2000; Okabe et al., 2013). MPOA lesions reduce maternal care in female rodents (rat: Noonan & Kristal, 1979; Terkel, Bridges, & Sawyer, 1979; Numan & Callahan, 1980; Fleming, Miceli, & Moretto, 1983; Franz, Leo, & Steuer 1986; Lee, Clancy, & Fleming, 1999; Numan et al., 1988; Olazábal et al., 2002; Stack et al., 2002; house mouse: Tsuneoka et al., 2013; Siberian hamster [*Mesocricetus*

auratus]: Miceli & Malsbury, 1982; California mouse: Lee & Brown, 2002, 2007), as does infusion of GABA agonists into the MPOA (rat: Arrati et al., 2006). Moreover, kindling of the MPOA increases female rats' preference for pup-associated environments in conditioned place-preference paradigms (Morgan, Watchus, & Fleming, 1997; Morgan et al., 1999).

The MPOA is also critical for paternal care in male rodents (Bales & Saltzman, 2016; Horrell, Hickmott, & Saltzman, 2018). MPOA lesions disrupt paternal care in male California mice (Lee & Brown, 2002, 2007) and disrupt or prevent sensitized allopaternal behavior in male rats and house mice (Rosenblatt, Hazelwood, & Poole, 1996; Sturgis & Bridges, 1997; Tsuneoka et al., 2015). Conversely, optogenetic activation of the MPOA decreases infanticide in male mice (Tsuneoka et al., 2015). Additionally, c-fos expression in the MPOA increases after exposure to pups in male house mice (Tsuneoka et al., 2015), prairie voles (*Microtus ochrogaster*; Kirkpatrick et al., 1994), North American deermice (*Peromyscus maniculatus*; Lambert et al., 2013), and California mice (Lambert et al., 2013; Horrell et al., 2017). California mouse fathers, but not virgins, display higher levels of c-fos in the MPOA after exposure to a pup than after exposure to a control stimulus (de Jong et al., 2009).

Changes in morphology of MPOA neurons are associated with the transition into motherhood, the hormonal milieu of pregnancy, and the extent of maternal care in female rodents (Gubernick, Sengelaub, & Kurz, 1993; Keyser-Marcus et al., 2001; Shams et al., 2012; Parent et al., 2017). Only one study has compared MPOA neural morphology between virgin males and fathers in any species: Gubernick, Sengelaub, and Kurz (1993) reported no differences in MPOA cross-sectional somal area between California mouse fathers and virgin males, with no other properties of neurons analyzed.

The electrophysiological properties of MPOA neurons have received little attention, especially in the context of parental care. Here we test the hypothesis that fatherhood increases intrinsic excitability, increases

synaptic excitation and/or decreases synaptic inhibition, and alters the morphology of MPOA neurons in California mice.

2. Materials and methods

2.1. Animals

Experiments were performed on young adult California mice that were born and maintained in our breeding colony at the University of California, Riverside and descended from mice purchased from the Peromyscus Genetic Stock Center (University of South Carolina, Columbia, SC, USA). Animals were housed in 44 x 24 x 20 cm polycarbonate cages containing aspen shavings and cotton wool for nesting material, with food (Purina Rodent Chow 5001) and water available *ad libitum*. Colony rooms were kept on a 14:10 light:dark cycle (lights on from 0500 h to 1900 h).

2.2. Experimental design

At 27-33 days of age, prior to the birth of the next litter of siblings, animals were removed from their parents' cage and housed in groups of three or four same-sex, age-matched littermates and/or unrelated juveniles. At sexual maturity (~3 months of age), each male mouse either remained in its group that was created at weaning (virgin males) or was paired with an unrelated female (fathers). Males were randomly assigned to the virgin and father conditions, except that those assigned to the two conditions were age-matched. Three to seven days after the birth of their first litter, fathers underwent a pup test followed by electrophysiological experiments (see below). Virgin males were tested in an age-matched fashion; age on the day of data collection did not differ between virgin males (162.1±9.4 days [mean ± SE]) and fathers (175.0±7.4 days [mean ± SE]; $p=0.283$, $df=37$). All animal procedures were consistent with the *Guide for the Care and Use of Animals* and were approved by the Institutional Animal Care and Use Committee of the

University of California, Riverside. All chemicals were purchased from Sigma-Aldrich (St. Louis, MO, USA) unless otherwise indicated.

2.3. Pup test

At 0900-1000 h, males were taken from their home cage and housed singly in a clean cage for 10 min. An unrelated, 1- to 5-day-old pup was then placed in the corner of the cage farthest from the male. The cage was video-recorded for 20 minutes, and the following behaviors were scored with The Observer software v. 11.5 (Noldus, Wageningen, Netherlands): latency to sniff the pup, latency to initiate paternal behavior (i.e., licking, grooming, or huddling), percent time spent sniffing the pup, percent time spent in paternal behavior, and percent time not in contact with the pup (i.e., not sniffing or engaging in paternal behavior). If a pup was attacked, the test was stopped, and the pup was immediately euthanized with pentobarbital, and the subject was assigned a score of 0 time spent in paternal behavior.

2.4. Preparation of MPOA slices for in vitro recording

Immediately after the behavioral test, the mouse was anesthetized with isoflurane until areflexic, and the brain was rapidly removed and placed into modified artificial cerebrospinal fluid (ACSF; in mM: KCl, 2.5; NaH_2PO_4, 1; $MgSO_4$, 1.3; $CaCl_2$, 2.5; $NaHCO_3$, 26.2; D-(+)-glucose, 11; Sucrose, 196.7; 3-morpholinopropane-1-sulfonic acid (MOPS), 3.5; sodium pyruvate, 2; kynurenic acid, 3; saturated with 95%O_2/5%CO_2). Coronal slices (300 μm-thick) were cut on a vibrating microtome (VT1000, Leica Biosystems Inc., Buffalo Grove, IL, USA). Sections containing the preoptic area were selected using easily identifiable landmarks (i.e., the anterior commissure and third ventricle) and incubated in the modified ACSF for at least 30 minutes. Slices were then transferred into standard ACSF for at least 30 minutes before

recording (in mM; NaCl, 119; KCl, 2.5; NaH_2PO_4, 1; $MgSO_4$, 1.3; $CaCl_2$, 2.5; $NaHCO_3$, 26.2; D-(+)-glucose, 11; saturated with 95%O_2/5%CO_2, osmolarity: 290-300 mOsm/L).

Electrophysiological data were obtained via blind whole-cell recording (Blanton, Turco, & Kriegstein, 1989) using patch electrodes with internal tip diameter of 1.5-2.5 μm. Patch electrodes were filled with either a Cs-based solution with QX-314 for recording synaptic currents or a K-based solution for recording intrinsic properties. The solutions consisted of (in mM): Cs-Gluconate or K-gluconate, 128; CsCl or KCl, 7**;** QX-314, 10; EGTA, 1; HEPES, 10; Mg-ATP, 2; Na-GTP, 0.2; biocytin, 0.1-0.2%; pH 7.0–7.4; osmolarity: 290-300 mOsm/L. Electrodes had tip resistances of 3-6 MΩ. Recordings were amplified using an Axoclamp 2B amplifier (Axon Instruments, Union City, CA, USA) in voltage-clamp or current-clamp mode, digitized at 15 kHz for synaptic currents and 40 kHz for intrinsic properties (National Instruments, Austin, TX, USA), and saved to the hard disk of a personal computer (Macintosh G4) using the IgorPro (Wavemetrics Inc., Lake Oswego, OR, USA) data acquisition system. Because the central MPOA has been strongly implicated in parental care (Tsuneoka et al., 2013; 2015), neurons were obtained in that region (Fig. 1A): 609.32 ± 16.68 μm (SE ± mean) ventral to the anterior commissure and 297.86 ± 11.15 μm (SE ± mean) lateral to the midline. Location of neurons did not differ between virgins (n=45 neurons) and fathers (n=51 neurons) with respect to the anterior commissure ($p=0.172$, $df=95$) or midline ($p=0.168$, $df=95$).

2.5. Acquisition and analysis of data on intrinsic electrophysiological properties

Neurons were current-clamped at -70 mV, and 500-ms square pulses of positive or negative current with intensities from sub- to supra-threshold were injected at 0.2 Hz.

Properties of single action potentials (APs; Fig. 1B, 1C) were measured using small supra-threshold injections that elicited one to a few spikes. The amplitude of single APs was measured from the inflection

point between the initial passive depolarization from the current injection and the beginning of the spike to the peak of the spike. The threshold was measured from baseline to the inflection point. Action potential half-width was measured as the duration of the AP at 50% of its amplitude. Fast afterhyperpolarizations (fAHPs) were quantified at two points: as the change in voltage from the inflection point to the minimal voltage 3-5 ms and 20-25 ms later.

Spike trains were obtained by increasing the magnitude of current injections. Maximum number of APs was measured as the highest number of APs resulting from any amount of injected current. Responses to positive injections of current that elicited spike trains were quantified by plotting the magnitude of the current injection (the input) and the resulting number of APs (the output). Input/Output (I/O) plots were well fit by an exponential function, the plateau of which was the modeled maximum number of APs and tau (τ) of which provided a measure of excitability (Fig. 3B). I/O plots were also created for average inter-spike interval (ISI) and current injected. From these I/O plots, minimum average ISI as well as tau were quantified to provide a metric of excitability independent of the maximum number of APs. Following a spike train, medium afterhyperpolarizations (mAHP) and slow afterhyperpolarizations (sAHP) were measured at -55 mV from baseline to peak of the hyperpolarization after the AP train and 450 ms after the offset of the AP train, respectively.

Properties of subthreshold responses to negative current injection were quantified. For subthreshold potentials, the peak amplitude and the amplitude at 400 ms of the current pulse (i.e., at steady-state) were determined for each current amplitude and plotted. These I/O plots were well fit by a straight line for both peak and steady-state measures, and the slopes of the lines were used as an overall measure of hyperpolarizing potential amplitude (Fig. 4).

2.6. Acquisition and analysis of data on post-synaptic currents (PSCs)

174 To quantify PSCs, stimulation was applied with a bipolar parylene-coated tungsten stimulating
175 electrode (FHC, Bowdoin, ME, USA; tip resistance ~1 MΩ; tip separation ~50 μm) placed ~200 um dorsal
176 to the recording electrode. Neurons were clamped at the chloride reversal potential (~-55 mV) to record
177 excitatory PSCs (EPSCs) and at the glutamate reversal (~0 mV) to record inhibitory PSCs (IPSCs). Single
178 pulses 100 μs in duration were delivered at varying intensities to attain minimal and maximal PSC
179 amplitude. Minimal PSC amplitude was operationalized as the current response using the greatest stimulus
180 intensity that resulted in a failure rate of >20%. Stimulus intensity was then increased incrementally until the
181 maximal PSC amplitude was reached. Stimulus intensity (the input) and the recorded PSC (the output) were
182 used to generate I/O curves. These I/O curves were well fit by a single exponential function and from these
183 exponential models, modeled maximum PSC amplitude was calculated.

184 Trains of PSCs were elicited by stimuli consisting of 10, 100 μs pulses at various inter-pulse intervals
185 (IPIs) of 10, 25, 50, 100, 200, 400 ms. For trains, stimulus intensity was adjusted to evoke PSCs of
186 approximately half the maximal PSC amplitude for that particular cell. For each train of PSCs, the paired-
187 pulse ratio (PPR) was defined as the ratio of the amplitude of the second PSC to the first; the steady-state
188 ratio (SSR) was defined as the ratio of the mean amplitude of the last 3 PSCs to the first.

189 Properties of spontaneous PSCs (sPSCs) were determined from unstimulated records of varying
190 durations. Typically, 30-50 spontaneous events were acquired for both EPSCs (when present) and IPSCs.
191 Spontaneous excitatory PSCs (sEPSCs) were recorded at -55mV. Spontaneous inhibitory PSCs (sIPSCs)
192 were recorded at 0 mV. Mean amplitude and frequency of sEPSCs and sIPSCs were determined.

193 *2.7. Acquisition and analysis of morphological data*

After recordings, slices were fixed in 10% formalin overnight at 4°C, rinsed in phosphate buffer (PB), then permeabilized in PB with 0.5% Triton X-100 and 5% goat serum for 30 min at room temperature. Slices were then incubated in a PB-based solution containing 5% goat serum and ALEXA-488 streptavidin (Molecular Probes; Eugene, OR, USA) at 0.01mg/mL overnight at 4°C. Sections were mounted in 90% glycerol with 4% *N*-propyl gallate added. Neurons were imaged using laser-scanning confocal microscopy (Zeiss 510). Images of dendrites were acquired at 10x with a 2x digital zoom. In all cases, the gain and black level were adjusted so that most of the labeled dendrites were saturated. Z-stacks were obtained for the entire depth of the cell, and 2-dimensional projections of neuronal morphology were derived using the maximal pixel intensity at each point in the X–Y plane. Dendritic morphology was analyzed using the Sholl analysis (Hickmott & Steen, 2005; Hickmott & Dinse, 2013). In this analysis, concentric circles were overlaid on an image of a neuron at 20 μm intervals centered on the soma; the number of intersections of each circle with labeled processes was determined for the entire neuron for a measure of overall neurite complexity. Quadrantized Sholl analyses for determination of a possible bias in dorsal-ventral and medial-lateral domains were conducted: Quadrant 1 (Q1) = dorsal medial, Q2 = dorsal lateral, Q3 = ventral medial, and Q4 = ventral lateral. In addition, number of branch points in each quadrant, total number of branch points, total neurite length, length of longest neurite, number of neurites leaving the soma, soma circumference, and largest soma diameter were measured. Properties of primary, secondary, and tertiary neurites were quantified. Primary neurites were defined as neurites leaving the soma, secondary neurites were defined as the shorter neurite process after a branch point on a primary neurite, and tertiary neurites were defined as the shorter neurite process after a branch point on a secondary neurite.

2.8. Statistical analyses

All data were analyzed using SPSS (IBM Corp, 2013), Microsoft Excel, or SAS. Normality was

tested using the Shapiro-Wilk test, and homogeneity of variance was tested using Levene's test. Depending on normality and homogeneity of variance, data from virgin males and fathers were compared using two-tailed Students' t-tests or Mann-Whitney U tests. Associations between behavioral and neuronal measures were evaluated using Spearman correlations. Multiple simultaneous tests involving related data, such as those in Supplemental Table 1, increase risk of Type 1 errors. To compensate, we used the positive False Discovery Rate procedure as implemented in SAS Procedure Multtest. That procedure indicated that none of the correlations reported in Supplemental Table 1 would be considered statistically significant after controlling for multiple comparisons. We refer to the three correlations with p values <0.05 as nominally significant.

3. Results

3.1. Pup test

Data on pup-directed behavior was available for 13 virgins and 33 fathers (Fig. 2). Fathers had a lower latency to sniff and initiate paternal behavior (licking, grooming, or huddling) than virgin males (sniff: U=114, p=0.014, paternal care: U=79, p=0.001). Additionally, fathers spent less time sniffing (U=118, p=0.019) more time in paternal behavior (U=110.5, p=0.011), and less time not in contact with pups (U=131.5, p=0.043).

3.2. Electrophysiology

For analysis of intrinsic properties, a total of 22 cells were patched in 15 virgin males and a total of 31 cells were patched in 25 fathers. For analysis of PSCs, a total of 22 cells were patched in 11 virgin males and 19 were patched in 12 fathers. Resting potential and input resistance did not differ between virgins and

fathers in the Cs-based solution used to measure PSCs or in the K-based solution used to measure intrinsic properties (Table 1).

3.2.1. Properties of action potentials

Voltage responses to 500 ms-long square pulses of positive and negative current of various intensities were acquired while cells were current-clamped at -70 mV. APs were evoked by positive currents, and the properties of single APs (Fig. 1B, 1C) and trains (Fig. 1D) were examined. Each neuron exhibited one of two general spiking patterns (Fig. 3): Regular-spiking (RS), in which the inter-spike intervals (ISIs) increased gradually during the train, and Fast-spiking (FS), in which ISIs did not change during the train. RS and FS cells were further divided into initial-bursting (IB) and non-initial-bursting, based on the presence or absence of a high-frequency burst of APs at the start of the train. Measurements of properties of single APs in initial-bursting cells were done on an AP not in the burst. Percentages of neurons in these spiking categories were similar in virgins and fathers (numbers of cells: FS: 9 virgin, 13 father; IB-FS: 2 virgin, 1 father; RS: 7 virgin, 13 father; IB-RS: 4 virgin, 4 father; $p=0.72$, Freeman-Halton extension of Fisher's exact test).

Initially, we compared all cells from virgins to those of fathers. None of the parameters extracted differed significantly between groups (Table 2).

Cells were then grouped into RS and FS groups, with IB cells subsumed into those categories, and properties of single APs (Table 3), trains of APs (Table 4), and responses to hyperpolarizing current (Table 5) were compared between virgins and fathers. Again, we found no significant differences, though the minimum average AP ISI tended to be longer in RS of fathers than in virgins (Table 4). The peak slope/steady-state slope tended to be greater in FS cells of fathers than in virgins (Table 5).

Finally, we grouped cells by spiking patterns (FS, IB-FS, RS, IB-RS) and compared properties of

single APs (Table 6), trains of APs (Table 7), and responses to hyperpolarizing current (Table 8) between virgins and fathers. IB-RS cells of fathers, compared to virgins, tended to have greater fAHP at 3-5 ms (Table 6). RS cells of fathers tended to have smaller maximum voltage change in response to hyperpolarizing current than RS cells of virgins (Table 8).

3.2.2. Properties of PSCs

Spontaneous PSCs and PSCs in response to local stimulation were characterized and compared in virgins and fathers. All cells exhibited inhibitory currents (n=41 cells from 23 animals), while a subset of cells exhibited both inhibitory and excitatory currents (n=29 cells from 19 animals). The percentage of cells in the two categories did not differ significantly between virgins (IPSC only: n=7, IPSC+EPSC: n=15) and fathers (IPSC only: n=5, IPSC+EPSC: n=14; p=0.74, Fisher's exact test). Representative traces of excitatory and inhibitory evoked PSCs are shown in Figure 5A. Virgins and fathers did not differ in maximal excitatory PSC amplitude, but fathers had significantly lower maximal inhibitory current than virgins (Fig. 5B, Table 9).

PPRs and SSRs of EPSCs and IPSCs did not differ at any inter-pulse interval, though we found a trend for fathers to have an increased EPSC PPR at 200-ms inter-pulse intervals as well as a strong trend for fathers to have a lower IPSC PPR at 10-ms inter-pulse intervals, compared to virgins (Fig. 7, Table 9). Virgins and fathers did not significantly differ in amplitude or frequency of spontaneous EPSCs or IPSCs, though was a trend for fathers to have less frequent sEPSCs (Fig. 6, Table 9).

3.3. Morphology

A total of 45 neuronal morphologies were captured: 23 from 17 virgins and 22 from 17 fathers (Fig. 8). Insufficient numbers of morphologies were captured to allow for comparisons between subtypes of

neurons based on spiking patterns, so tests were conducted between metrics of virgins and fathers (Table 10). No differences were found in quantified morphological properties, though we found a trend for fathers to have shorter average length of primary neurites than virgins (Table 10).

3.4. *Correlations of neural and behavioral measurements*

Spearman correlations were run between two key behavioral metrics (i.e., latency to engage in paternal behavior and percent time spent in paternal care) and neural properties in virgins, which exhibited more variability in paternal behavior than fathers. Latency to engage in parental behavior showed nominally significant negative correlations with AP amplitude ($r_s(14)=-0.682$, $p=0.007$) and largest soma diameter ($r_s(7)=-0.954$, $p=0.001$), and a nominally significant positive correlation with maximum voltage change in response to a hyperpolarizing stimulus ($r_s(14)=0.67$, $p=0.009$). Thus, the more readily a virgin male engaged in paternal behavior toward the pup, the larger his AP amplitude and maximal soma diameter, and the smaller his maximum voltage change in response to a hyperpolarizing stimulus. However, after correcting for multiple comparisons, none of these correlations were statistically significant (see Supplemental Table 1 for full correlation results). Time spent in paternal care did not correlate with any neuronal properties.

4. Discussion

The MPOA plays a role in parental care in males and/or females in multiple vertebrate clades (Demski & Knigge, 1971; Slawski & Buntin, 1995; Tsuneoka et al., 2015). The identity of the cells involved in parental care, categorized by gene expression, afferent or efferent connectivity, or morphological or electrophysiological profiles, is under investigation but not well understood (e.g., Lonstein & De Vries, 2000; Cservenák et al., 2013; 2017; Tsuneoka et al., 2013; Dobolyi et al., 2014; Kuroda & Numan, 2014; Wu et al., 2014). Recently, neurons in the central MPOA have been implicated in paternal care in mice

(Tsuneoka et al., 2013, 2015). In order to attain a thorough, unbiased survey of electrophysiological and morphological profiles of central MPOA neurons potentially involved in paternal care, we used blind, whole-cell recording to characterize all neurons in a non-specific manner in the central MPOA of both virgin males and fathers in the biparental California mouse. This experiment is among the first to characterize the electrophysiological properties of MPOA neurons in males of any species, and the first to attempt to relate these properties explicitly to paternal behavior.

The MPOA of California mice likely contains a multitude of cell types. We observed four major spiking patterns in cells of the central MPOA: fast-spiking (FS), initial-bursting fast-spiking (IB-FS), regular-spiking (RS), and initial-bursting regular-spiking (IB-RS) (Fig. 3). Initial-bursting cells characteristically fired a cluster of action potentials at stimulus onset. Regardless of presence or absence of an initial burst, cells could show accommodation (regular-spiking cells) or no accommodation (fast-spiking cells). Similar spiking patterns have been observed in neocortex, and their genetic determinants are starting to be understood (for review see Markram et al., 2004). Comparisons of intrinsic electrophysiological properties of trains and single action potentials between virgins and fathers in our study revealed no significant differences in any cell type. The numerous trends for differences in intrinsic electrophysiological properties in MPOA cells suggest that plasticity may be occurring in specific cells types categorized by connectivity or gene expression. Input resistances were similar to those reported in a nearly analogous slice preparation performed in mice by Lundius et al (2010).

Both spontaneous PSCs and PSCs evoked by stimulating ~200 μms dorsal to the recording electrode were characterized and compared between virgins and fathers. As in rat MPOA, both excitatory (EPSCs) and inhibitory (IPSCs) currents were observed (Hoffman et al., 1994; Hoffman, Wuarin, & Dudek, 1994; Karlsson, Haage, & Johansson, 1997; Sundgren-Andersson & Johansson, 1998; Haage & Johansson, 1999).

322 Fathers exhibited lower maximal evoked IPSCs than virgins, suggesting decreased inhibition in the MPOA
323 in fathers. Since the maximally-evoked IPSC was affected, it is likely that the overall number of inhibitory
324 synapses onto MPOA cells was reduced. This might be caused by mating, cohabitation with a (pregnant)
325 female, experience with pups, and/or a number of hormonal changes that occur during the transition into
326 fatherhood in California mice (reviewed below). Frequency of spontaneous PSCs was similar to that
327 reported in mice by Lundius et al. (2010).

328 The observed reduction in inhibition is consistent with the previously documented increase in
329 excitability of the MPOA in fathers (de Jong et al., 2009; but see Horrell et al., 2017). How exactly the
330 reduction in inhibition affects specific behaviors is unclear, in part because the source of inhibition is
331 unknown. Many studies on the input to the MPOA have been conducted (e.g., Simerly & Swanson, 1986;
332 Miller & Lonstein, 2009; Rondini et al., 2010; Been & Petrulis, 2011; Northcutt & Lonstein, 2011; Sanathara
333 et al., 2014). Unfortunately, the inhibitory inputs onto cells of the MPOA are poorly characterized and not
334 easily separated into distinct terminal fields that would allow stimulation of identifiable axon terminals in
335 this preparation. There are certainly inhibitory inputs from both intrinsic interneurons and from extrinsic
336 sources, including strong projections from other parts of the hypothalamus, bed nucleus of the stria
337 terminalis, and amygdala (e.g., Fenske et al., 1975; Gardener & Phillips, 1977; Mayer, 1981; Coolen &
338 Wood, 1998; Pardo-Bellver et al., 2012; Shimogawa et al., 2015; Lebow & Chen, 2016; Kohl et al., 2018).
339 Further studies using optogenetic activation of identified terminal fields in slices or *in vivo* could help
340 resolve this important question.

341 MPOA neurons in rats exhibit inhibitory currents mediated by $GABA_A$ and glycine receptors (Haage
342 & Johansson, 1999; Hoffman et al., 1994; Hoffman, Wuarin, & Dudek, 1994; Karlsson, Haage, &
343 Johansson, 1997) as well as excitatory currents mediated by AMPA and NMDA glutamate receptors and

likely by T-, L-, N-, P- and Q–type Ca^{+2} channels (Hoffman, Wuarin, & Dudek, 1994; Karlsson et al., 1997; Sundgren-Andersson & Johansson, 1998; Malinina, Druzin, & Johansson, 2010; Tabarean et al., 2005; Qiu et al., 2006). Some of these currents in preoptic area neurons are acutely altered by estradiol (Qiu et al., 2006; Druzin et al., 2011; Zhang et al., 2013; Rønnekleiv et al., 2015), allopregnanolone (Haage & Johansson, 1999; Haage, Bäckström, & Johansson, 2002; 2005), testosterone derivatives (Oberlander et al., 2012), capsaicin (Karlsson et al., 2005), and serotonin (Lee et al., 2008).

If and how these chemicals act on preoptic area neurons to alter paternal care in male California mice is a promising area of research. Testosterone increases paternal behavior in California mice via aromatization to estrogen, and fathers in this species have more aromatase activity in the MPOA than mated males without pups (Trainor and Marler, 2001, 2002; Trainor et al., 2003). Reports of fathers having lower circulating levels of testosterone and dihydrotestosterone (DHT) than mated males, and lower circulating DHT than virgin males, as well as the inability of DHT to restore paternal care after castration, further implicate the increase in aromatase activity and estrogen signaling in the MPOA as important for paternal care in this species (Trainor and Marler, 2002; Trainor et al., 2003; but see Gubernick & Nelson, 1989). Furthermore, estrogen implants in the MPOA of male rats increase paternal care (Rosenblatt and Ceus, 1998). Progesterone, which is metabolized to allopregnanolone, is lower in California mouse fathers than in virgin males (Trainor et al., 2003), and progesterone antagonism increases while progesterone administration decreases paternal care in house mice (Schneider et al., 2003). Additionally, the effects of prolactin and oxytocin on paternal care and on MPOA neurons in California mice merit investigation, as circulating levels of these peptides may change across the reproductive cycle in males of this species (Gubernick & Nelson, 1989; Gubernick et al., 1995). The possibility that hormonal effects on neural properties differ with reproductive status (e.g., virgin or father) is a potential avenue for future studies.

Some aspects of the morphology of MPOA cells (specifically, soma size and dendritic branching) of female rats are altered by pregnancy and attendant endocrine changes (i.e., progesterone withdrawal followed by elevated estrogen levels) (Keyser-Marcus et al., 2001). Female California mice show a similar increase in somal area during the transition into motherhood (Gubernick et al., 1993). In a recent study of MPOA neuronal morphology in rats, mothers that licked and groomed their pups at high levels had fewer branches on primary dendrites than low-licking-grooming mothers; however, no differences were found in Sholl analysis, total dendritic arbor length, number of spines, and number of primary dendrites (Parent et al., 2017). Only one previous study has characterized MPOA properties in male California mice. MPOA volume, number of neurons, density of neurons, and somal area did not differ among fathers, estranged fathers (fathers removed from their mate and pups 5 days postpartum for 45 days), and virgin males, according to a Golgi-Cox stain (Gubernick et al., 1993). Similarly, no major effects of fatherhood were seen in morphology of MPOA neurons in the present study. Fathers did, however, show a trend for reduction in the average length of primary neurites. Analysis of morphology of neurons of a specific cell type, such as cells that express estrogen receptors or the neuropeptide galanin, is a promising avenue of research (Kohl et al., 2018).

Overall, the findings of this study suggest that some plasticity occurs in the MPOA during the transition into fatherhood and the onset of paternal behavior in male California mice, particularly decreased inhibition. Future studies targeting specific cell types in the MPOA, categorized on the basis of gene expression or connectivity, are needed and may reveal plasticity that facilitates parental behavior (e.g., Kohl et al., 2018; McHenry et al., 2017). Characterization and manipulation of particular inputs to the MPOA such as those from the medial amygdala, bed nucleus of the stria terminalis, periaqueductal grey, as well as hypothalamic stress and aggression centers may be of interest. Characterization of plasticity induced by hormones and neuropeptides implicated in parental behavior via signaling in the MPOA, as well as experience-dependent plasticity in the MPOA, may elucidate important mechanisms of parental care.

Acknowledgements

We thank the staff of the UCR Life Science and Spieth Hall Vivaria, Dr. Akiko Sato for care of the animals, and members of the Saltzman lab and Hickmott lab, especially Liliana Gonzalez, Diane Luu, Anastasia Shakhbazova, and Corinne Blaine, for assistance with the animal colony and experiments. We also thank Dr. Theodore Garland, Jr. for assistance with statistical analyses, and Dr. B.C. Trainor and an anonymous reviewer for very constructive comments on an earlier draft of the manuscript.

Funding: This work was supported by a UC Riverside Academic Senate grant to PWH, and grants from the National Institutes of Health (R21HD075021) and National Science Foundation (IOS-1256572) to WS.

399 **References**

400 Arrati PG, Carmona C, Dominguez G, Beyer C, Rosenblatt JS (2006). GABA receptor agonists in the medial
401 preoptic area and maternal behavior in lactating rats. Physiol Behav 87:51-65.

402 Bales KL, Saltzman W (2016) Fathering in rodents: neurobiological substrates and consequences for
403 offspring. Horm Behav 77:249-259.

404 Been LE, Petrulis A (2011) Chemosensory and hormone information are relayed directly between the medial
405 amygdala, posterior bed nucleus of the stria terminalis, and medial preoptic area in male Syrian
406 hamsters. Horm Behav 59:536-548.

407 Blanton MG, Lo Turco JJ, Kriegstein AR (1989) Whole cell recording from neurons in slices of reptilian and
408 mammalian cerebral cortex. J Neurosci Methods 30:203-210.

409 Coolen LM, Wood RI (1998) Bidirectional connections of the medial amygdaloid nucleus in the Syrian
410 hamster brain: simultaneous anterograde and retrograde tract tracing. J Comp Neurol 399:189-209.

411 Cservenák M, Kis V, Keller D, Dimén D, Menyhárt L, Oláh S, Szabó ER, Barna J, Renner E, Usdin TB,
412 Dobolyi A (2017) Maternally involved galanin neurons in the preoptic area of the rat. Brain Struct
413 Funct 222:781-798.

414 Cservenák M, Szabó ÉR, Bodnár I, Lékó A, Palkovitis M, Nagy GM, Usdin TB, Dobolyi A (2013) Thalamic
415 neuropeptide mediating the effects of nursing on lactation and maternal motivation.
416 Psychoneuroendocrinology 38:3070-3084.

417 de Jong TR, Chauke M, Harris BN, Saltzman W (2009) From here to paternity: neural correlates of the onset

418 of paternal behavior in California mice (*Peromyscus californicus*). Horm Behav 56:220-231.

419 Demski LS, Knigge KM (1971) The telencephalon and hypothalamus of the bluegill (*Lepomis macrochirus*):
420 Evoked feeding, aggressive and reproductive behavior with representative frontal sections. J Comp
421 Neurol 143:1-16.

422 Dobolyi A, Grattan DR, Stolzenberg DS (2014) Preoptic inputs and mechanisms that regulate maternal
423 responsiveness. J Neuroendocrinol 26:627-640.

424 Druzin M, Malinina E, Grimsholm O, Johansson S (2011) Mechanism of estradiol-induced block of voltage-
425 gated K⁺currents in rat medial preoptic neurons. PLoS One 6:e20213.

426 Dudley D (1974) Contributions of paternal care to the growth and development of the young in *Peromyscus*
427 *californicus*. Behav Biol 11:155-166.

428 Dulac C, O'Connell LA, Wu Z (2014) Neural control of maternal and paternal behaviors. Science 345:765-
429 770.

430 Denske M, Ellendorff F, Wuttke W (1975) Response of medial preoptic neurons to electrical stimulation of
431 the mediobasal hypothalamus, amygdala and mesencephalon in normal, serotonin or catecholamine
432 deprived female rats. Exp Brain Res 22:495-507.

433 Fleming AS, Miceli M, Moretto D (1983) Lesions of the medial preoptic area prevent the facilitation of
434 maternal behavior produced by amygdala lesions. Physiol Behav 31:503-510.

435 Franz JR, Leo RJ, Steuer MA, Kristal MB (1986) Effects of hypothalamic knife cuts and experience on
436 maternal behavior in the rat. Physiol Behav 38:629-640.

437 Gardner CR, Phillips SW (1977) The influence of the amygdala on the basal septum and preoptic area of the
438 rat. Exp Brain Res 29:249-263.

439 Gubernick DJ, Alberts JR (1987) The biparental care system of the California mouse, *Peromyscus*
440 *californicus*. J Comp Psychol 101:169-177.

441 Gubernick DJ, Nelson R (1989). Prolactin and paternal behavior in the biparental California mouse,
442 *Peromyscus californicus*. Horm Behav 23:203–210.

443 Gubernick DJ, Sengelaub DR, Kurz EM (1993) A neuroanatomical correlate of paternal and maternal
444 behavior in the biparental California mouse *Peromyscus californicus*. Behav Neurosci 107:194-201.

445 Gubernick DJ, Teferi T (2000) Adaptive significance of male parental care in a monogamous mammal. Proc
446 Biol Sci 267:147-150.

447 Gubernick DJ, Winslow JT, Jensen P, Jeanotte L, Brown J (1995) Oxytocin changes males over the
448 reproductive cycle in the monogamous, biparental California Mouse, *Peromyscus californicus*. Horm
449 Behav 29:59-73.

450 Haage D, Johansson S (1999) Neurosteroid modulation of synaptic and GABA-evoked current in neurons
451 from the rat medial preoptic nucleus. J Neurophysiol 82:143-151.

452 Haage D, Bäckström T, Johansson S (2002) Allopregnanolone modulates spontaneous GABA release via
453 presynaptic CL- permeability in rat preoptic nerve terminals. Brain Res 958:405-413.

454 Haage D, Bäckström T, Johansson S (2005) Interaction between allopregnanolone and pregnenolone sulfate
455 in modulating GABA-mediated synaptic currents in neurons from the rat medial preoptic nucleus.

Brain Res 1033:58-67.

Hickmott P, Dinse H (2013) Effects of aging on properties of the local circuit in rat primary somatosensory cortex (S1) in vitro. Cereb Cortex 23:2500-2513.

Hickmott PW, Steen PA (2005) Large-scale changes in dendritic structure during reorganization of adult somatosensory cortex. Nat Neurosci 8:140-142.

Hoffman NW, Kim YI, Gorski A, Dudek FE (1994) Homogeneity of intracellular electrophysiological properties in different neuronal subtypes in medial preoptic slices containing the sexually dimorphic nucleus of the rat. J Comp Neurol 345:396–408.

Hoffman NW, Wuarin JP, Dudek EF (1994) Whole-cell recordings of spontaneous synaptic currents in medial preoptic neurons from rat hypothalamic slices: mediation by amino acid neurotransmitters. Brain Res 660:349–352.

Horrell ND, Hickmott PW, Saltzman W (2018) Neural regulation of paternal behavior in mammals: sensory, neuroendocrine, and experiential influences on the paternal brain. Curr Top Behav Neurosci. doi: 10.1007/7854_2018_55

Horrell ND, Perea-Rodriguez JP, Harris BN, Saltzman W (2017) Effects of repeated pup exposure on behavioral, neural, and adrenocortical responses to pups in male California mice (*Peromyscus californicus*). Horm Behav 90:56-63.

Karlsson U, Haage D, Johansson S (1997) Currents evoked by GABA and glycine in acutely dissociated neurons form rat medial preoptic nucleus. Brain Res 770:256-260.

475 Karlsson U, Sundgren- Andersson AK, Näsström, Johansson S (1997) Glutamate-evoked currents in acutely
476 dissociated neurons from the rat medial preoptic nucleus. Brain Res 759:270-276.

477 Karlsson U, Sundgren-Andersson AK, Johansson S, Krupp JJ (2005) Capsaicin augments synaptic
478 transmission in the rat medial preoptic nucleus. Bran Res 1043:1-11.

479 Keyser-Marcus L, Stafisso-Sandoz G, Gerecke K, Jasnow A, Nightingale L, Lambert KG, Gatewood J,
480 Kinsley CH (2001) Alterations of medial preoptic area neurons following pregnancy and pregnancy-
481 like steroidal treatment in the rat. Brain Res Bull 55:737-745.

482 Kirkpatrick B, Kim JW, Insel TR (1994) Limbic system fos expression associated with paternal behavior.
483 Brain Res 658:112-118.

484 Kleiman DG, Malcom JR (1981) The evolution of male parental investment in mammals. In: Parental care in
485 mammals (1, ed), pp347-387. New York, NY: Plenum Publishing Corp.

486 Kohl J, Babayan BM, Rubinstein ND, Autry AE, Marin-Rodriguez B, Kapoor V, Miyamishi K, Zweifel LS,
487 Luo L, Uchida N and Dulac C (2018) Functional circuit architecture underlying parental behavior.
488 Nature 556: 326-331.

489 Komisaruk BR, Rosenblatt JS, Barona ML, Chinapen S, Nissanov J, O'Bannon RT, Johnson BM, Del Cerro
490 MC (2000) Combined c-fos and 14C-2-deoxyglucose method to differentiate site-specific excitation
491 from disinhibition: analysis of maternal behavior in the rat. Brain Res 859:262-272.

492 Kuroda KO, Numan M (2014) The medial preoptic area and the regulation of parental behavior. Neurosci
493 Bull 30:862-865.

494 Lambert KG, Franssen CL, Hampton JE, Rzucidlo AM, Hyer MM, True M, Kaufman C, Bardi M. (2013)
495 Modeling paternal attentiveness: distressed pups evoke differential neurobiological and behavioral
496 responses in paternal and nonpaternal mice. Neuroscience 234:1-12.

497 Lebow MA, Chen A (2016) Overshadowed by the amygdala: the bed nucleus of the stria terminalis emerges
498 as key to psychiatric disorders. Mol Psychiatry 21:450-463.

499 Lee AW, Brown RE (2002) Medial preoptic lesions disrupt parental behavior in both male and female
500 California mice (*Peromyscus californicus*). Behav Neurosci 116:968-975.

501 Lee AW, Brown RE (2007) Comparison of medial preoptic, amygdala, and nucleus accumbens lesions on
502 parental behavior in California mice (*Peromyscus californicus*). Physiol Behav 92:617-628.

503 Lee AW, Clancy S, Fleming AS (1999) Mother rats bar-press for pups: effects of lesions of the mpoa and
504 limbic sites on maternal behavior and operant responding for pup-reinforcement. Behav Brain Res
505 108:215-231.

506 Lee JJ, Hahm ET, Lee CH, Cho YW (2008) Serotonergic modulation of GABAergic and
507 glutamatergic synaptic transmission in mechanically isolated rat medial preoptic area
508 neurons. Neurophyschopharmacology 33:340-352.

509 Lundius EB, Sanchez-Alavez M, Ghochani Y, Klaus J, Tabarean IV (2010). Histamine influences
510 body temperature by acting at H1 and H3 receptors on distinct populations of preoptic neurons. J
511 Neurosci 30:4369-4381.

512 Lonstein JS, De Vries GJ (2000) Maternal behaviour in lactating rats stimulates c-fos in glutamate
513 decarboxylase-synthesizing neurons of the medial preoptic area, ventral bed nucleus of the stria
514 terminalis, and ventrocaudal periaqueductal gray. Neuroscience 100:557-568.

515 Malinina E, Druzin M, Johansson S (2010) Differential control of spontaneous and evoked GABA release by
516 presynaptic L-type Ca^{2+} Channels in the rat medial preoptic nucleus. J Neurophysiol 104:200-209.

517 Markram H, Toledo-Rodriguez M, Wang Y, Gupta A, Silberberg G, Wu C (2004) Interneurons of the
518 neocortical inhibitory system. Nature Rev Neurosci 5:793-807.

519 Mayer ML (1981) Electrophysiological analysis of inhibitory synaptic mechanisms in the preoptic area of
520 the rat. J Physiol 316:327-346.

521 McHenry JA, Otis JM, Rossi MA, Robinson JE, Kosyk O, Miller NW, McElligott ZA, Budygin EA,
522 Rubinow DR, Stuber GD (2017) Hormonal gain control of a medial preoptic area social reward
523 circuit. Nat Neurosci 20:449-458.

524 Miceli MO, Malsbury CW (1982) Sagittal knife cuts in the near and far lateral preoptic area-hypothalamus
525 disrupt maternal behaviour in female hamsters. Physiol Behav 28:856-867.

526 Miller SM, Lonstein JS (2009) Dopaminergic projections to the medial preoptic area of postpartum rats.
527 Neuroscience 159:1384-1396.

528 Morgan HD, Watchus JA, Fleming AS (1997) The effects of electrical stimulation of the medial preoptic
529 area and the medial amygdala on maternal responsiveness in female rats. Ann N Y Acad Sci 807:602-
530 605.

531 Morgan HD, Watchus JA, Milgram NW, Fleming AS (1999) The long lasting effects of electrical simulation
532 of the medial preoptic area and medial amygdala on maternal behavior in female rats. Behav Brain
533 Res 99:61-73.

534 Noonan M, Kristal MB (1979) Effects of medial preoptic lesions on placentophagia and on the onset of
535 maternal behavior in the rat. Physiology Behavior 22:1197-1202.

536 Northcutt KV, Lonstein JS (2011) Neuroanatomical projections of the species-specific tyrosine hydroxylase-
537 immunoreactive cells of the male prairie vole bed nucleus of the stria terminalis and medial
538 amygdala. Brain Behav Evol 77:176-192.

539 Numan M (2006) Hypothalamic neural circuits regulating maternal responsiveness toward infants. Behav
540 Cogn Neurosci Rev 5:163-190.

541 Numan M (2014) Neurobiology of social behavior: toward an understanding of the prosocial and antisocial
542 brain. Cambridge, MA: Academic Press.

543 Numan M, Callahan EC (1980) The connections of the medial preoptic region and maternal behavior in the
544 rat. Physiol Behav 25:653-665.

545 Numan M, Corodimas KP, Numan MJ, Factor EM, Piers WD (1988) Axon-sparing lesions of the preoptic
546 region and substantia innominata disrupt maternal behavior in rats. Behav Neurosci 102:381-396.

547 Numan M, Insel TR (2003) The neurobiology of parental behavior. New York: Springer.

548 Oberlander JG, Porter DM, Onakomaiya MM, Penatti CAA, Vithlani M, Moss SJ, Clark AS, Henderson LP.
549 Estrous cycle variation in $GABA_A$receptor phosphorylation enable rapid modulation by anabolic

androgenic steroids in the medial preoptic area. Neuroscience 226:397-410.

Okabe S, Nagasawa M, Kihara T, Kato M, Harada T, Koshida N, Mogi K, Kikusui T (2013) Pup odor and ultrasonic vocalizations synergistically stimulate maternal attention in mice. Behav Neurosci 127:432-438.

Olazábal DE, Kalinichev M, Morrell JI, Rosenblatt JS (2002) MPOA cytotoxic lesions and maternal behavior in the rat: effects of midpubertal lesions on maternal behavior and the role of ovarian hormones in maturation of MPOA. Horm Behav 41:126-138.

Pardo-Bellver C, Cadiz-Moretti B, Novejarque A, Martinez-Garcia F, Lanuza E (2012) Differential efferent projections of the anterior, posteroventral, and posterodorsal subdivisions of the medial amygdala in mice. Front Neuroanat 6:33.

Parent C, Wen X, Dhir SK, Ryan R, Diorio J, Zhang TY (2017) Maternal care associates with differences in morphological complexity in the medial preoptic area. Behav Brain Res 326:22-32.

Qiu J, Bosch MA, Jamali K, Xue C, Kelly MJ, Rønnekleiv OK (2006) Estrogen upregulates T-type calcium channels in the hypothalamus and pituitary. J Neurosci 26:11072-11082.

Ribble DO (1991) The monogamous mating system of *Peromyscus californicus* as revealed by DNA fingerprinting. Behav Ecol Sociobiol 29:161-166.

Ribble DO, Salvioni M (1990) Social organization and nest co-occupancy in *Peromyscus californicus*, a monogamous rodent. Behav Ecol Sociobiol 26:9-15.

Rondini TA, Donato J, Rodrigues Bde C, Bittencourt JC, Elias CF (2010) Chemical identity and connections

of medial preoptic area neurons expressing melanin-concentrating hormone during lactation. J Chem Neuroanat 39:51-62.

Rønnekleiv OK, Zhang C, Bosch MA, Kelly MJ (2015) Kisspeptin and GnRH neuronal excitability: molecular mechanisms driven by 17β-Estradiol. Neuroendocrinology 102:184-193.

Rosenblatt JS, Ceus K (1998) Estrogen implants in the medial preoptic area stimulate maternal behavior in male rats. Horm Behav 33:23-30.

Rosenblatt JS, Hazelwood S, Poole J (1996) Maternal behavior in male rats: effects of medial preoptic area lesions and presence of maternal aggression. Horm Behav 30:201-215.

Sanathara NM, Moreas J, Mahavongtrakul M, Sinchak K (2014) Estradiol upregulates progesterone receptor and orphanin FQ colocalization in arcuate nucleus neurons and opioid receptor-like receptor-1 expression in proopiomelanocortin neurons that project to the medial preoptic nucleus in the female rat. Neuroendocrinology 100:103-118.

Schneider JS, Stone MK, Wynne-Edwards KE, Horton TH, Lydon J, O'Malley B, Levine JE (2003) Progesterone receptors mediate male aggression toward infants. Proc Natl Acad Sci U S A 100:2951-2956.

Shams S, Pawluski JL, Chatterjee-Chakraborty M, Oatley H, Mastroianni A, Fleming AS (2012) Dendritic morphology in the striatum and hypothalamus differentially exhibits experience-dependent changes in response to maternal care and early social isolation. Behav Brain Res 233:79-89.

Shimogawa Y, Sakuma Y, Yamanouchi K (2015) Efferent and afferent connections of the ventromedial hypothalamic nucleus determined by neural tracer analysis: implications for lordosis regulation in

589 female rats. Neurosci Res 91:19-33.

590 Simerly RB, Swanson LW (1986) The organization of neural inputs to the medial preoptic nucleus of the rat.
591 J Comp Neurol 246:312-342.

592 Slawski BA, Buntin JD (1995) Preoptic area lesions disrupt prolactin-induced parental feeding behavior in
593 ring doves. Horm Behav 29:148-166.

594 Stack EC, Balakrishnan R, Numan MJ, Numan M (2002) A functional neuroanatomical investigation of the
595 role of the medial preoptic area in neural circuits regulating maternal behavior. Behav Brain Res
596 131:17-36.

597 Sturgis JD, Bridges RS (1997) N-Methyl-DL-aspartic acid lesions of the medial preoptic area disrupt
598 ongoing parental behavior in male rats. Physiol Behav 62:305-310.

599 Sundgren-Andersson AK, Johansson S (1998) Calcium spikes and calcium currents in neurons from the
600 medial preoptic nucleus of rat. Brain Res 783:194-209.

601 Tabarean IV, Conti B, Behrens M, Korn H, Bartfai T (2005) Electrophysiological properties and
602 thermosensitivity of mouse preoptic and anterior hypothalamic neurons in culture.
603 Neuroscience 135:433-449.

604 Terkel J, Bridges RS, Sawyer CH (1979) Effects of transecting lateral neural connections of the medial
605 preoptic area on maternal behavior in the rat: nest building, pup retrieval and prolactin secretion.
606 Brain Res 169:369-380.

607 Trainor BC, Marler CA (2001) Testosterone, paternal behavior, and aggression in the
608 monogamous California mouse (*Peromyscus californicus*). Horm Behav 40:32–42.

609 Trainor BC, Marler CA (2002) Testosterone promotes paternal behaviour in a monogamous mammal via
610 conversion to oestrogen. Proc R Soc Lond B 269:823–829.

611 Trainor BC, Bird M, Alday MA, Schlinger BA, Marler CA, (2003) Variation in aromatase activity in the
612 medial preoptic area and plasma progesterone is associated with the onset of paternal behavior.
613 Neuroendocrinology 78:36–44.

614 Tsuneoka Y, Maruyama T, Yoshida S, Nishimori K, Kato T, Numan M, Kuroda KO (2013) Functional,
615 anatomical, and neurochemical differentiation of medial preoptic area subregions in relation to
616 maternal behavior in the mouse. J Comp Neurol 521:1633-1663.

617 Tsuneoka Y, Tokita K, Yoshihara C, Amano T, Esposito G, Huang AJ, Yu LM, Odaka Y, Shinozuka K,
618 McHugh TJ, Kuroda KO (2015) Distinct preoptic-BST nuclei dissociate paternal and infanticidal
619 behavior in mice. EMBO J 34:2652-2670.

620 Woodroffe R, Vincent A (1994) Mother's little helpers: Patterns of male care in mammals. Trends Ecol Evol
621 9:294-297.

622 Wu Z, Autry AE, Bergan JF, Watabe-Uchida M, Dulac CG (2014) Galanin neurons in the medial preoptic
623 area govern parental behavior. Nature 509:325-330.

624 Zhang C, Tonsfeldt KJ, Qiu J, Bosch MA, Kobayashi K, Steiner RA, Kelly MJ, and Rønnekleiv OK
625 (2013) Molecular mechanisms that drive estradiol-dependent burst firing of Kiss1 neurons in the rostral

periventricular preoptic area. Am J Physiol Endocrinol Metab 305:E1384-E1397.

628 **Figure Legends**

629 Figure 1. Medial preoptic area of hypothalamus (MPOA) and properties of single action potentials (APs). A)
630 Representative photomicrograph of 300 μm-thick coronal section used for recordings. The box, centered on
631 the third ventricle, approximately delineates the MPOA. The dashed box represents the approximate area
632 where recordings were made. AC: anterior commissure. B-C) Properties of single APs, including depictions
633 of threshold, amplitude, half width and fast afterhyperpolarizations (fAHPs). fAHPs were quantified as the
634 largest voltage difference from baseline to 3-5 ms and 20-25 ms after the action potential crossed the
635 baseline voltage. D) Depictions of medium afterhyperpolarization (mAHPs) and slow afterhyperpolarization
636 (sAHP) after a train of APs. mAHP was quantified as the lowest voltage from baseline after train offset, and
637 sAHP was quantified as voltage difference from baseline at 450 ms after stimulus offset.

638

639 Figure 2. Infant-directed behavior of virgin males (n=13) and fathers (n=33). A) Box and whisker plots of
640 time spent in each behavior. Fathers spent significantly more time in paternal behaviors (licking, grooming,
641 and/or huddling pup), less time sniffing, and less time not in contact with pups compared to virgins. B)
642 Latency to engage in pup-directed behaviors. Fathers approached pups and initiated paternal care
643 significantly more rapidly than did virgins. * $P < 0.05$.

644

645 Figure 3. Representative action potential (AP) trains of different cell types in the central medial preoptic
646 area. A) Fast-spiking (FS), in which inter-spike intervals (ISIs) do not change during the train, and regular-
647 spiking (RS), in which ISIs increase gradually during the train. RS and FS cells could also be initial-bursting
648 (IB), in which cells fired a short burst of APs at high frequency followed by an increased ISI. B) Example of

649 an input/output plot depicting the number of APs evoked by discrete amounts of depolarizing current (black
650 squares). An exponential function was fitted to the data (black line); from this line, τ and a modeled
651 maximum number of APs were determined.

652

653 Figure 4. Properties of responses to hyperpolarizing current injections. A) Example of voltage responses to
654 hyperpolarizing current steps of 500 ms duration. Responses at maximal hyperpolarization (peak) and at 400
655 ms (steady-state) were quantified for each step. B-C) Examples of input/output plots for discrete amounts of
656 hyperpolarizing current and resulting voltage changes from baseline to peak hyperpolarizing voltage
657 response (B) and to the response at 400 ms (i.e., at steady-state, C). The slopes of lines of best fit were
658 quantified.

659

660 Figure 5. Evoked postsynaptic currents (PSCs) in virgin males and fathers. A) Representative traces of an
661 excitatory postsynaptic current (bottom) and inhibitory postsynaptic current (top). B) Maximal PSCs in cells
662 from virgins (white, n=22) and fathers (gray, n=19). See Table 9 for full analysis of PSCs.

663

664 Figure 6. Spontaneous postsynaptic currents (PSCs) in virgin males and fathers. A) Representative traces of
665 spontaneous excitatory postsynaptic current (top) and inhibitory postsynaptic currents (bottom). B) Average
666 amplitude of spontaneous postsynaptic currents (sPSCs) of cells from virgins (white; excitatory sPSCs:
667 n=10; inhibitory sPSCs: n=21) and fathers (gray; excitatory sPSCs: n=5; inhibitory sPSCs: n=13). C)

668 Frequency of sPSCs in cells from virgins (white; excitatory sPSCs: n=10; inhibitory sPSCs: n=21) and
669 fathers (gray; excitatory sPSCs: n=6; inhibitory sPSCs: n=13).

670

671 Figure 7. Postsynaptic currents (PSCs) evoked by trains of stimuli at various interpulse intervals (IPIs). A)
672 PSCs in response to stimulation at various IPIs (indicated between traces in ms). Cell were voltage-clamped
673 at 0 mV to isolate inhibitory postsynaptic currents and at -55mV to isolate excitatory postsynaptic currents.
674 Note change in scale from top three traces to bottom three traces. B) Paired-pulse ratios and steady-state
675 ratios of PSCs evoked at various IPIs. No differences were observed between virgin males (white) and
676 fathers (gray) at any IPI. See Table 9 for full analysis of PSCs.

677

678 Figure 8. Examples of MPOA neurons filled with biocytin during whole-cell recordings. Quadrantized Sholl
679 analysis revealed no differences in morphology between cells from virgin males (white, n=23) and fathers
680 (gray, n= 22). See Table 10 for more detailed morphological analyses.
681

682

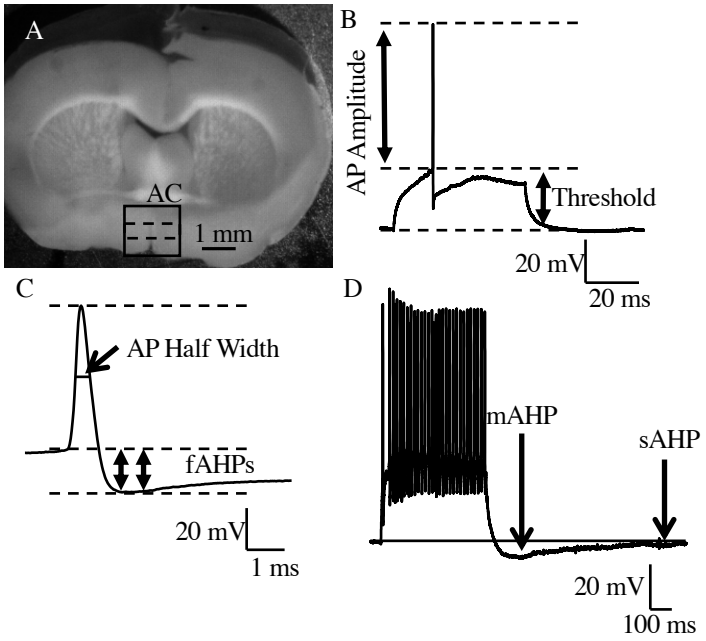
A
AC
1 mm
B
AP Amplitude
Threshold
20 mV
20 ms
C
AP Half Width
fAHPs
20 mV
1 ms
D
mAHP
sAHP
20 mV
100 ms

Figure 1

A

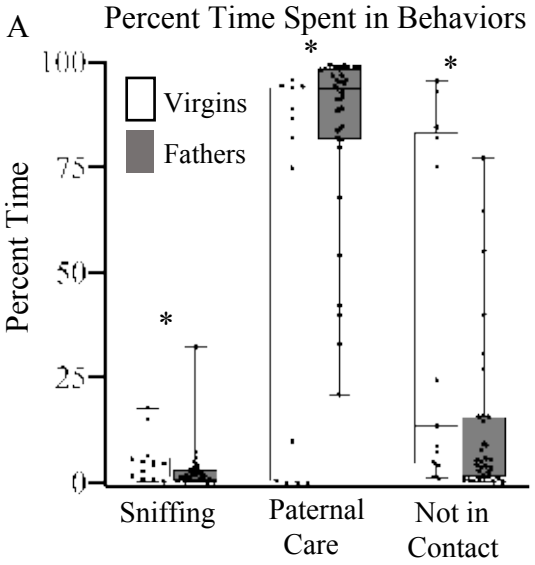
Percent Time Spent in Behaviors
Percent Time
100
75
50
25
0
Virgins
Fathers
Sniffing
Paternal Care
Not in Contact

B

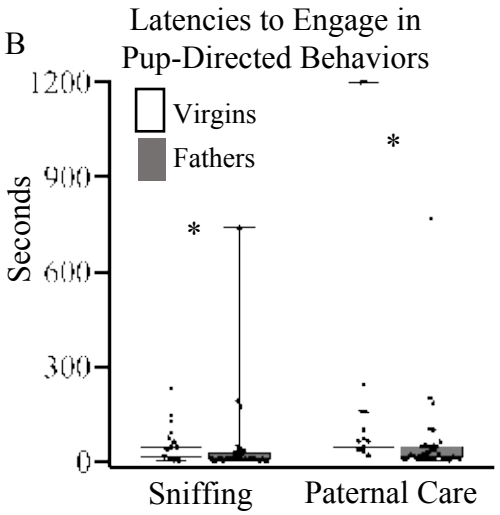
Latencies to Engage in Pup-Directed Behaviors
Seconds
1200
900
600
300
0
Virgins
Fathers
Sniffing
Paternal Care

Figure 2

Figure 3

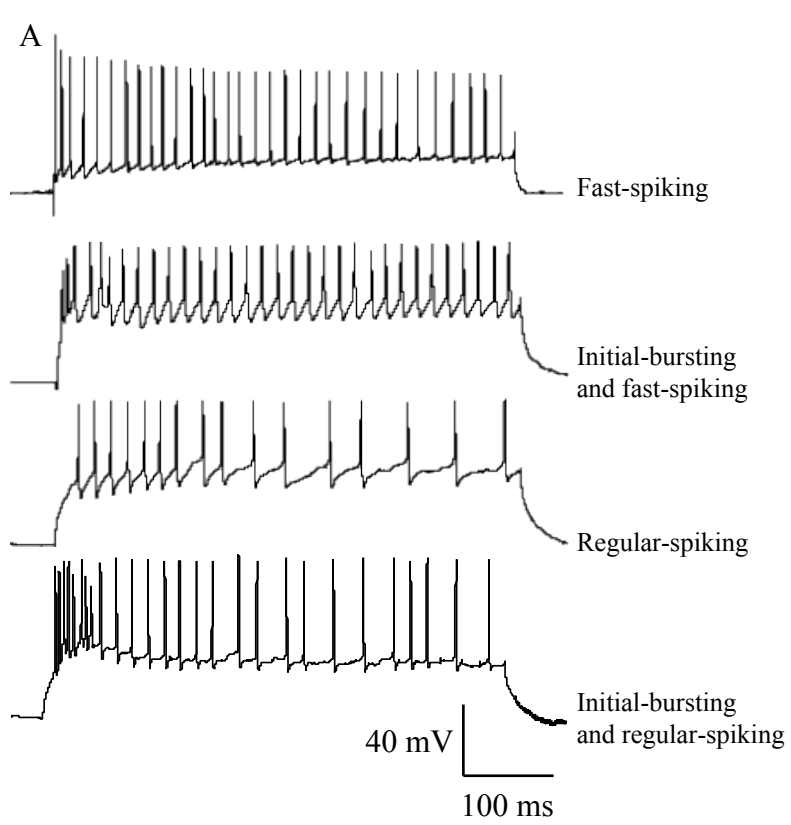
A
Fast-spiking
Initial-bursting
and fast-spiking
Regular-spiking
Initial-bursting
and regular-spiking
40 mV
100 ms

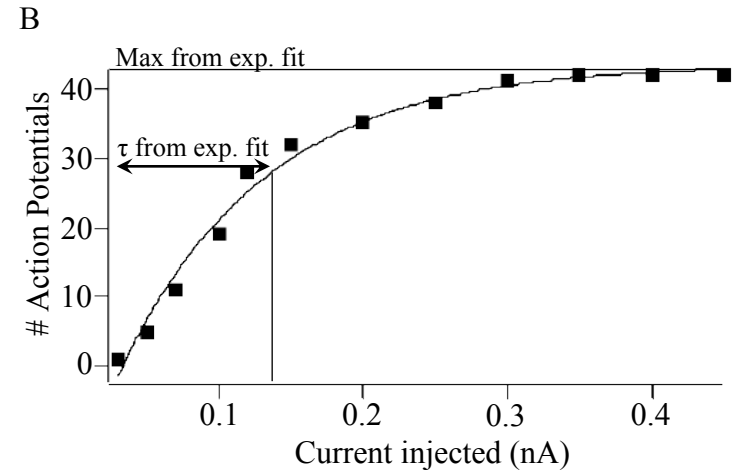
B
Max from exp. fit
τ from exp. fit
Action Potentials
0
10
20
30
40
0.1
0.2
0.3
0.4
Current injected (nA)

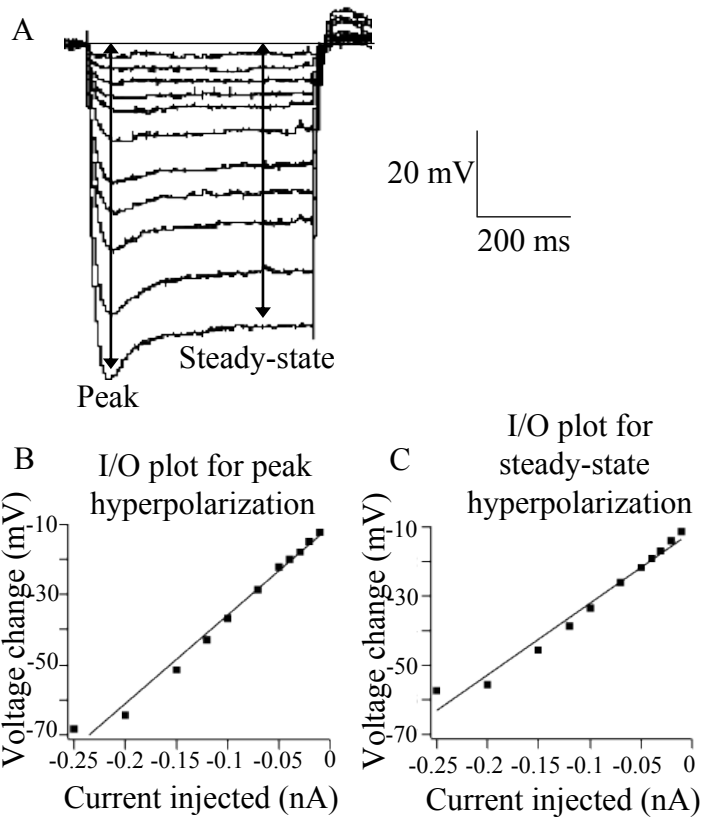
A
20 mV
200 ms
Steady-state
Peak
B
I/O plot for peak hyperpolarization
Voltage change (mV)
-10
-30
-50
-70
-0.25 -0.2 -0.15 -0.1 -0.05 0
Current injected (nA)
C
I/O plot for steady-state hyperpolarization
Voltage change (mV)
-10
-30
-50
-70
-0.25 -0.2 -0.15 -0.1 -0.05 0
Current injected (nA)

Figure 4

A

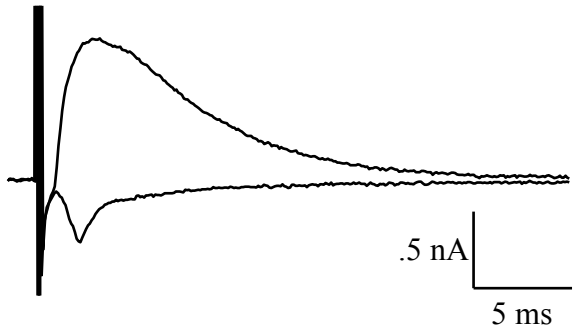

B

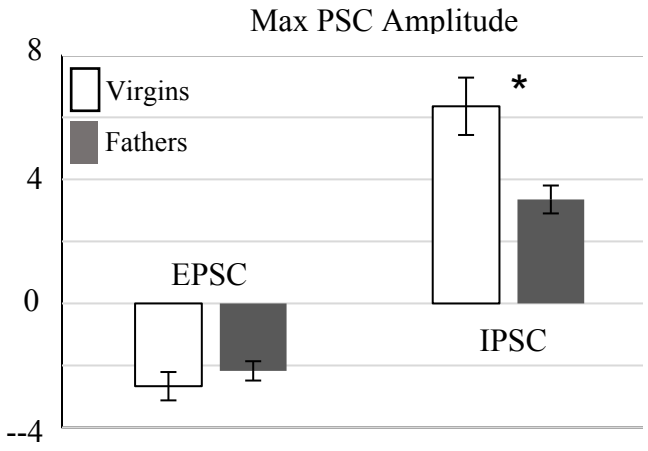

Figure 5

A

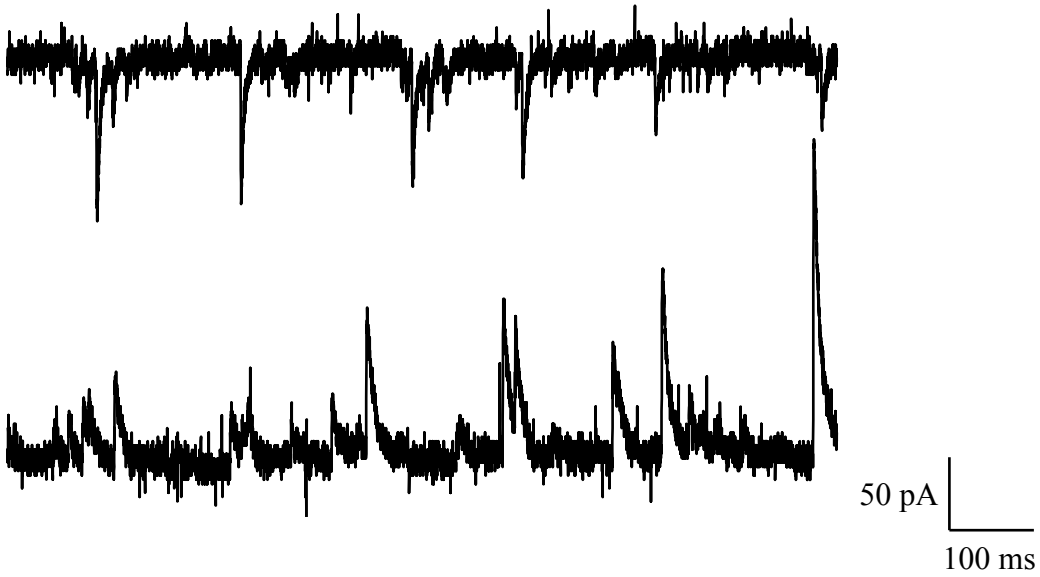
50 pA
100 ms

Figure 6

B

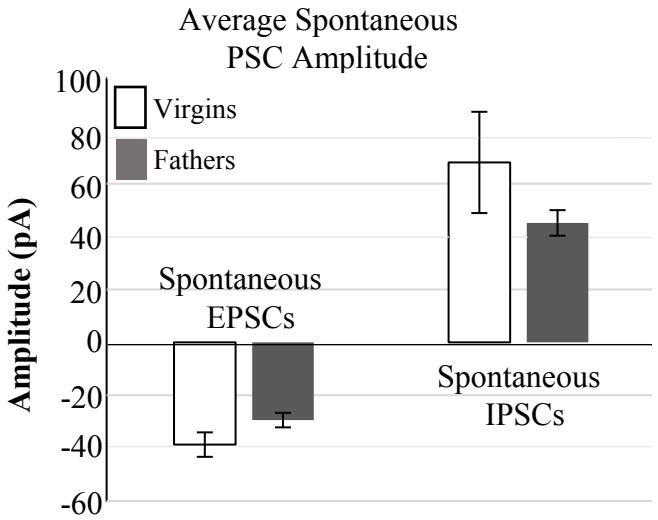
Average Spontaneous
PSC Amplitude
Amplitude (pA)
100
80
60
40
20
0
-20
-40
-60
Virgins
Fathers
Spontaneous
EPSCs
Spontaneous
IPSCs

C

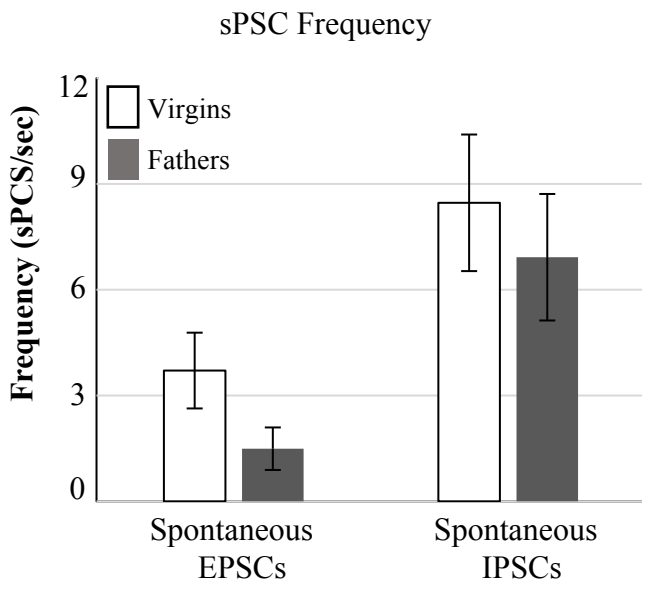
sPSC Frequency
Frequency (sPCS/sec)
12
9
6
3
0
Virgins
Fathers
Spontaneous
EPSCs
Spontaneous
IPSCs

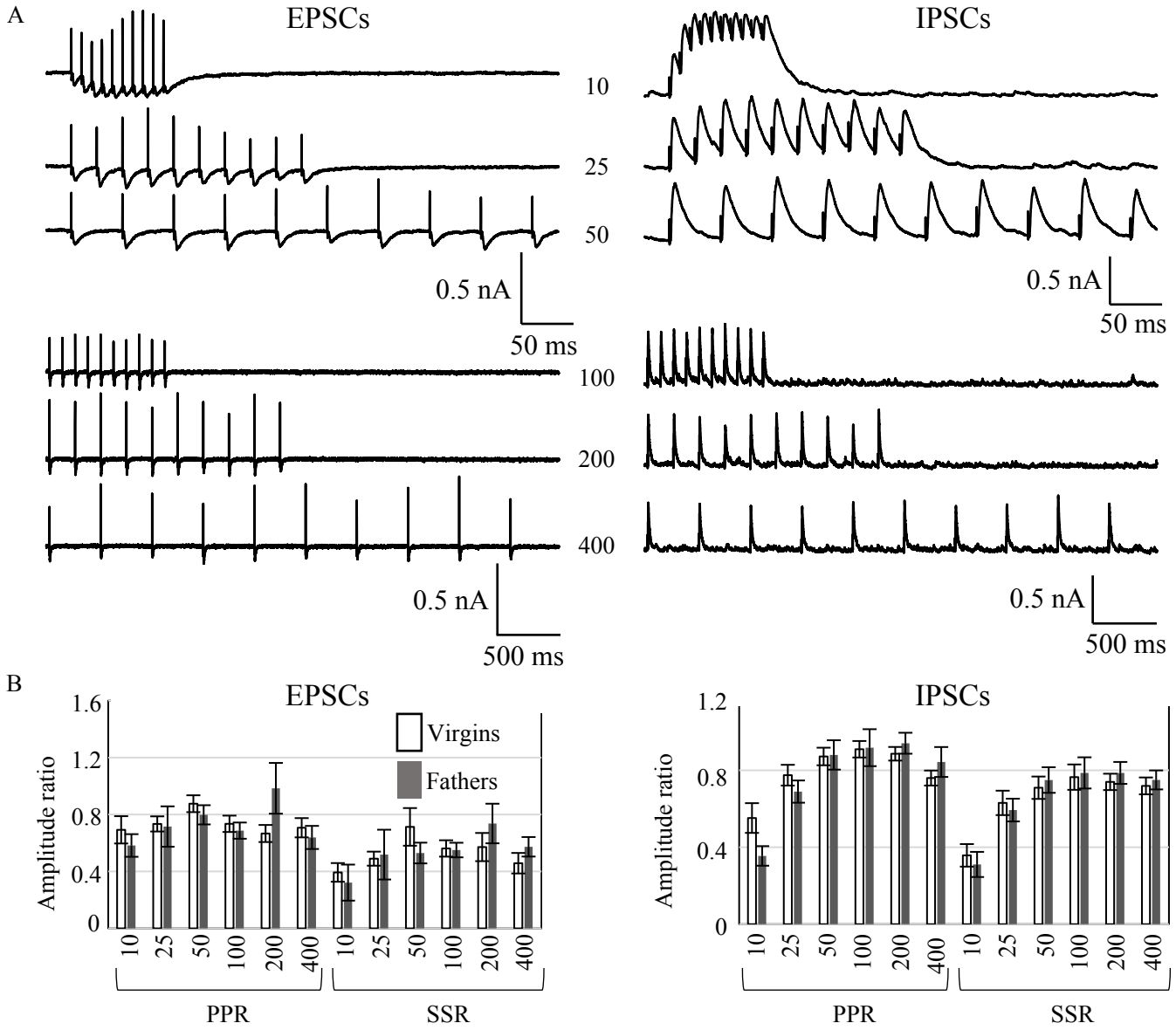
A
EPSCs
IPSCs
10
25
50
100
200
400
0.5 nA
50 ms
0.5 nA
50 ms
0.5 nA
500 ms
0.5 nA
500 ms
B
EPSCs
IPSCs
Virgins
Fathers
Amplitude ratio
1.6
1.2
0.8
0.4
0
1.2
0.8
0.4
0
10
25
50
100
200
400
PPR
SSR

Figure 7

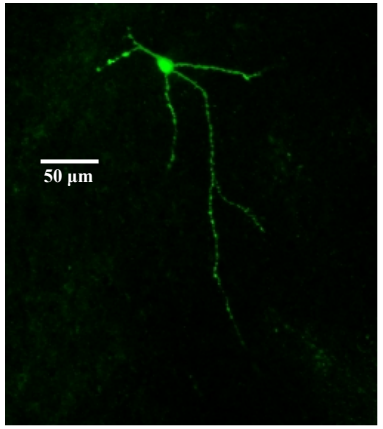

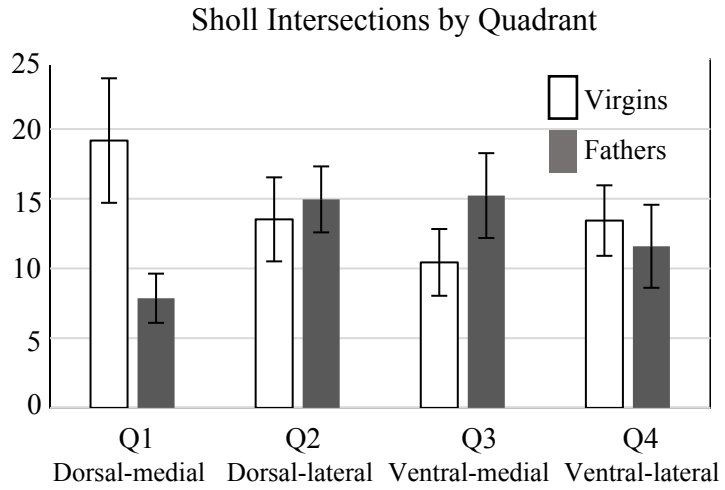

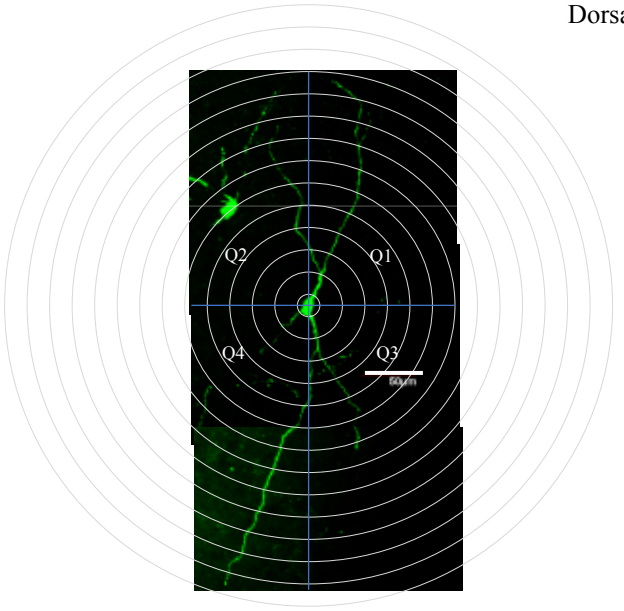

Figure 8

* Color should be used for this figure*

Table 1. Resting potential and input resistance of neurons from virgin males and fathers in Cs-based and K-based solutions.

		Virgins			Fathers			Analysis			
Property	Unit	N	Mean	SE	N	Mean	SE	Test	df	t	P-value
Resting potential											
Cs-based solution	mV	22	-44.50	1.09	19	-45.95	1.32	t-test	39	0.85	0.40
K-based solution	mV	23	-50.17	1.72	32	-44.63	3.66	t-test	53	0.23	0.23
Input resistance											
Cs-based solution	MΩ	22	519.45	40.08	19	567.47	48.10	t-test	49	-0.77	0.44
K-based solution	MΩ	23	648.56	60.00	31	812.35	77.66	t-test	52	-1.57	0.12

A Cs-based solution with QX-314 was used for recording synaptic currents, and a K-based solution was used for recording intrinsic properties (see Materials & Methods). N = number of cells.

Table 2. Properties of action potentials and responses to hyperpolarizing current in all cell types in virgin males and fathers.

		Virgins			Fathers			Analysis			
Measure	Unit	N	Mean	SE	N	Mean	SE	Test	df	Stat.	P-value
Properties of single APs											
Threshold	mV	22	29.29	1.80	31	27.74	1.64	t-test	51	0.63	0.53
Amplitude	mV	22	40.89	3.92	31	45.64	2.79	t-test	51	-1.02	0.31
Half-width	ms	22	0.92	0.09	32	0.85	0.05	MW	--	324.0	0.76
fAHP at 3-5 ms	mV	22	-11.24	1.24	31	-10.46	1.11	t-test	51	-0.46	0.64
fAHP at 20-25 ms	mV	22	-10.74	1.29	31	-8.68	0.97	MW	--	289.0	0.35
Properties of trains of APs											
Maximum # of APs	#	21	45.86	2.57	32	52.53	4.61	MW	--	335.0	0.99
Maximum APs from exp. fit	#	21	80.13	12.96	31	76.27	9.66	MW	--	295.0	0.57
Tau from AP exp. fit	nA	21	0.40	0.15	32	0.24	0.04	MW	--	334.0	0.97
Minimum average AP ISI	ms	21	10.32	0.83	32	12.26	1.06	MW	--	279.0	0.30
Minimum ISI from exp. fit	ms	21	16.06	3.31	32	12.18	1.44	MW	--	312.0	0.66
Tau from ISI exp. fit	ms	21	0.03	0.01	32	0.39	0.32	MW	--	287.0	0.37
mAHP	mV	20	-3.56	1.05	30	-3.35	0.70	MW	--	273.5	0.60
sAHP	mV	19	-2.20	0.38	30	-2.31	0.36	t-test	47	0.20	0.84
Responses to hyperpolarizing current											
Maximum voltage change	mV	21	-90.74	6.76	28	-76.46	5.50	t-test	47	-1.65	0.10
Slope of peak hyperpolarization	---	21	45.19	6.06	30	40.30	4.30	MW	--	313.0	0.97
Slope of steady-state hyperpolarization	---	21	38.95	6.13	30	34.89	3.91	MW	--	301.0	0.79

Peak slope/steady-state slope	---	21	1.14	0.04	30	1.18	0.03	MW	--	250.0	0.21

N = number of cells, AP = action potential, ISI = inter-spike interval, fAHP = fast afterhyperpolarization, mAHP = medium afterhyperpolarization, sAHP = slow afterhyperpolarization, exp. = exponential, Stat. = test statistic, MW = Mann-Whitney U test.

Table 3. Properties of single action potentials in fast-spiking and regular-spiking cells in virgin males and fathers.

		Virgins			Fathers			Analysis			
Property	Unit	N	Mean	SE	N	Mean	SE	Test	df	t	P-value
Fast-spiking											
Threshold	mV	11	26.16	2.02	14	24.22	1.77	t-test	23	0.73	0.48
Amplitude	mV	11	43.44	5.50	14	49.17	4.93	t-test	23	-0.77	0.45
Half-width	ms	11	0.77	0.11	14	0.79	0.09	t-test	23	-0.12	0.90
fAHP at 3-5 ms	mV	11	-11.79	2.01	14	-11.27	1.79	t-test	23	-0.19	0.85
fAHP at 20-25 ms	mV	11	-12.49	2.22	14	-8.80	1.18	t-test	23	-1.56	0.13
Regular-spiking											
Threshold	mV	11	32.43	2.76	17	30.63	2.43	t-test	26	0.48	0.64
Amplitude	mV	11	38.34	5.74	17	42.74	3.05	t-test	26	-0.74	0.47
Half-width	ms	11	1.06	0.15	17	0.91	0.04	t-test	26	1.12	0.25
fAHP at 3-5 ms	mV	11	-10.68	1.53	17	-9.79	1.41	t-test	26	-0.42	0.68
fAHP at 20-25 ms	mV	11	-8.99	1.20	17	-8.58	1.51	t-test	26	-0.19	0.85

N = number of cells, fAHP = fast afterhyperpolarization.

Table 4. Properties of trains of action potentials of fast-spiking and regular-spiking cells in virgin males and fathers.

		Virgins			Fathers			Analysis			
Property	Unit	N	Mean	SE	N	Mean	SE	Test	df	Stat.	P-value
Fast-spiking											
Maximum APs	#	10	48.2	4.38	15	62.93	7.13	MW	--	57.5	0.33
Maximum APs from exp. fit	#	10	62.09	7.39	14	74.13	10.43	MW	--	65.0	0.77
Tau from AP exp. fit	nA	10	0.19	0.05	15	0.19	0.04	MW	--	75.0	1.00
Minimum average AP ISI	ms	10	9.85	1.42	15	9.77	1.22	t-test	23	0.42	0.97
Minimum ISI from exp. fit	ms	10	19.60	6.58	15	11.68	1.50	MW	--	58.0	0.35
Tau from ISI exp. fit	ms	10	0.03	0.01	15	0.03	0.004	MW	--	74.0	0.96
mAHP	mV	10	-2.70	1.77	14	-2.87	0.68	t-test	22	0.10	0.92
sAHP	mV	9	-1.66	0.50	14	-2.11	0.47	t-test	21	0.64	0.53
Regular-spiking											
Maximum APs	#	11	43.73	2.94	17	43.35	5.21	MW	--	76.0	0.41
Maximum APs from exp. fit	#	11	96.53	23.24	17	78.04	15.68	MW	--	76.0	0.41
Tau from AP exp. fit	nA	11	0.60	0.27	17	0.29	0.07	MW	--	89.0	0.83
Minimum average AP ISI	ms	11	10.74	0.98	17	14.46	1.51	t-test	26	-1.82	0.08*
Minimum ISI from exp. fit	ms	11	12.85	2.06	17	12.62	2.40	t-test	26	0.07	0.95
Tau from ISI exp. fit	ms	11	0.04	0.01	17	0.70	0.60	MW	--	65.0	0.18
mAHP	mV	10	-4.43	1.15	16	-3.76	1.18	MW	--	63.0	0.37
sAHP	mV	10	-2.69	0.53	16	-248	0.54	t-test	24	-0.27	0.79

N = number of cells, AP = action potential, ISI = inter-spike interval, fAHP = fast afterhyperpolarization, mAHP = medium afterhyperpolarization, sAHP = slow afterhyperpolarization, exp. = exponential, Stat. = test statistic, MW = Mann-Whitney U test.

* = $0.10 > p > 0.05$.

Table 5. Responses to hyperpolarizing current in fast-spiking and regular-spiking cells in virgin males and new fathers.

		Virgins			Fathers			Analysis			
Property	Unit	N	Mean	SE	N	Mean	SE	Test	df	Stat.	P-value
Fast-spiking											
Maximum voltage change	mV	10	-89.31	9.44	14	-76.50	8.47	t-test	22	-1.00	0.33
Slope of peak hyperpolarization	---	10	42.86	10.44	14	34.95	5.36	MW	--	63.0	0.68
Slope of steady-state hyperpolarization	---	10	40.87	11.04	14	30.19	5.02	MW	--	60.0	0.56
Peak slope/steady-state slope	---	10	1.09	0.04	14	1.20	0.06	MW	--	40.0	0.08*
Regular-spiking											
Maximum voltage change	mV	11	-92.04	10.05	14	-76.41	7.35	t-test	23	-1.27	0.21
Slope of peak hyperpolarization	---	11	42.49	7.15	16	44.98	6.48	t-test	25	-0.15	0.88
Slope of steady-state hyperpolarization	---	11	37.20	6.55	16	39.01	5.84	t-test	25	-0.20	0.84
Peak slope/steady-state slope	---	11	1.19	0.07	16	1.16	0.03	MW	--	88.0	1.00

Responses to 500 ms-long square pulses of positive and negative current of various intensities were acquired while cells were current-clamped at -70 mV (see Material and Methods). N = number of cells, Stat. = test statistic, MW = Mann-Whitney U test. * = $0.10 > p > 0.05$.

Table 6. Properties of single action potentials for fast-spiking, initial-bursting + fast-spiking, regular-spiking, and initial-bursting + regular-spiking cells in virgin males and fathers.

		Virgins			Fathers			Analysis[a]			
Property	Unit	N	Mean	SE	N	Mean	SE	Test	df	Stat.	P-value
Fast-spiking											
Threshold	mV	9	25.90	2.41	12	23.43	1.98	t-test	19	0.80	0.43
Amplitude	mV	9	42.55	6.36	12	48.89	5.37	t-test	19	-0.76	0.45
Half-width	ms	9	0.86	0.11	12	0.79	0.10	t-test	19	0.42	0.68
fAHP at 3-5 ms	mV	9	-11.73	2.40	12	-10.80	2.01	t-test	19	-0.30	0.77
fAHP at 20-25 ms	mV	9	-13.21	2.53	12	-8.73	1.39	t-test	19	-1.66	0.11
Initial-bursting + fast-spiking											
Threshold	mV	2	27.30	---	2	28.97	---	---	---	---	---
Amplitude	mV	2	47.45	---	2	50.83	---	---	---	---	---
Half-width	ms	2	0.4	---	2	0.78	---	---	---	---	---
fAHP at 3-5 ms	mV	2	-12.05	---	2	-14.14	---	---	---	---	---
fAHP at 20-25 ms	mv	2	-9.25	---	2	-9.20	---	---	---	---	---
Regular-spiking											
Threshold	mV	6	32.88	4.66	13	29.39	3.03	t-test	17	0.64	0.53
Amplitude	mV	6	42.27	8.39	13	42.74	3.51	t-test	17	-0.06	0.95
Half-width	ms	6	1.06	0.24	13	0.89	0.05	MW	--	30.5	0.46
fAHP at 3-5 ms	mV	6	-12.45	1.86	13	-9.36	1.76	t-test	17	-1.07	0.30
fAHP at 20-25 ms	mV	6	-7.55	1.57	13	-9.32	0.97	t-test	17	1.00	0.33
Initial-bursting + regular-spiking											

Threshold	mV	4	31.83	3.89	4	34.67	2.71	MW	--	6.0	0.56
Amplitude	mV	4	26.79	5.65	4	42.73	7.15	t-test	6	-1.75	0.13
Half-width	ms	4	1.19	0.12	4	0.96	0.06	t-test	6	1.82	0.12
fAHP at 3-5 ms	mV	4	-6.29	0.94	4	-11.18	1.98	t-test	6	2.23	0.07*
fAHP at 20-25 ms	mV	4	-10.02	2.01	4	-6.21	6.11	t-test	6	-0.59	0.57

N = number of cells, fAHP= fast afterhyperpolarization, Stat. = test statistic, MW = Mann-Whitney U test. [a] Properties of initial-bursting + fast-spiking cells were not analyzed statistically due to small sample sizes. * = $0.10 > p > 0.05$.

Table 7. Properties of trains of action potentials for fast-spiking, initial-bursting + fast-spiking, regular-spiking, and initial-bursting + regular-spiking cells in virgin males and fathers.

		Virgins			Fathers			Analysis[a]			
Property	Unit	N	Mean	SE	N	Mean	SE	Test	df	Stat.	P-value
Fast-spiking											
Maximum APs	#	8	50.88	5.06	13	62.23	7.73	MW	--	40.0	0.39
Maximum APs from exp. fit	#	8	62.80	9.13	12	76.00	11.67	t-test	18	-0.82	0.43
Tau from AP exp. fit	nA	8	0.14	004	13	0.21	0.05	MW	--	36.0	0.25
Minimum average AP ISI	ms	8	8.79	1.56	13	9.85	1.30	MW	--	47.0	0.72
Minimum ISI from exp. fit	ms	8	20.16	8.31	13	11.98	1.61	MW	--	45.0	0.61
Tau from ISI exp. fit	ms	8	0.03	0.01	13	0.03	0.005	MW	--	48.0	0.77
mAHP	mV	8	-2.47	2.13	13	-2.80	0.86	t-test	19	0.174	0.86
sAHP	mV	7	-1.81	0.60	13	-2.02	0.50	t-test	18	0.25	0.80
Initial-bursting + fast-spiking											
Maximum APs	#	2	37.5	---	2	61	---	---	---	---	---
Maximum APs from exp. fit	#	2	59.23	---	1	35.35	---	---	---	---	---
Tau from AP exp. fit	nA	2	0.35	---	2	0.07	---	---	---	---	---
Minimum average AP ISI	ms	2	14.05	---	2	9.25	---	---	---	---	---
Minimum ISI from exp. fit	ms	2	17.37	---	2	9.701	---	---	---	---	---
Tau from ISI exp. fit	ms	2	0.04	---	2	0.03	---	---	---	---	---
mAHP	mV	1	-7.3	---	1	-3.9	---	---	---	---	---
sAHP	mV	1	-2.2	---	1	-3.3	---	---	---	---	---
Regular-spiking											
Maximum APs	#	6	46.83	4.17	13	43.61	6.27	t-test	17	0.33	0.75

Maximum APs from exp. fit	#	6	111.04	38.08	13	73.39	15.87	MW	--	26.0	0.25
Tau from AP exp. fit	nA	6	0.62	0.39	13	0.25	0.06	MW	--	34.0	0.66
Minimum average AP ISI	ms	6	10.38	1.41	13	13.94	1.71	t-test	17	-1.31	0.21
Minimum ISI from exp. fit	ms	6	11.23	1.93	13	13.01	3.10	t-test	17	-0.37	0.72
Tau from ISI exp. fit	ms	6	0.04	0.01	13	0.84	0.79	MW	--	37.0	0.86
mAHP	mV	6	-5.73	1.78	13	-3.01	0.79	t-test	17	-1.63	0.12
sAHP	mV	6	-1.84	0.76	13	-2.54	0.63	t-test	17	0.65	0.53
Initial-bursting + regular-spiking											
Maximum APs	#	4	42.5	3.78	4	42.5	10.25	t-test	6	0.00	1.0
Maximum APs from exp. fit	#	4	92.24	28.36	4	93.16	46.89	MW	--	7.00	0.77
Tau from AP exp. fit	nA	4	0.72	0.50	4	0.42	0.24	MW	--	7.00	0.77
Minimum average AP ISI	ms	4	13.32	1.26	4	16.13	3.55	t-test	6	-1.01	0.35
Minimum ISI from exp. fit	ms	4	16.81	3.47	4	11.35	2.20	MW	--	4.00	0.25
Tau from ISI exp. fit	ms	4	0.03	0.02	4	0.23	0.15	MW	--	2.00	0.83
mAHP	mV	4	-3.01	1.80	4	-6.01	4.32	t-test	6	0.64	0.55
sAHP	mV	4	-3.97	0.51	4	-2.28	1.16	MW	--	5.00	0.39

N = number of cells, AP = action potential, ISI = inter-spike interval, fAHP = fast afterhyperpolarization, mAHP = medium afterhyperpolarization, sAHP = slow afterhyperpolarization, exp. = exponential, Stat. = test statistic, MW = Mann-Whitney U test.

[a] Properties of initial-bursting + fast-spiking cells were not analyzed statistically due to small sample sizes.

Table 8. Responses to hyperpolarizing current for fast-spiking, initial-bursting + fast-spiking, regular-spiking, and initial-bursting + regular-spiking cells in virgin males and fathers.

		Virgins			Fathers			Analysis[a]			
Property	Unit	N	Mean	SE	N	Mean	SE	Test	df	Stat.	P-value
Fast-spiking											
Max voltage change	mV	8	-94.01	10.91	13	-74.16	8.79	t-test	19	-1.41	0.18
Slope of peak hyperpolarization	---	8	46.96	12.69	13	34.99	5.79	MW	--	43.0	0.52
Slope of steady-state hyperpolarization	---	8	46.0	13.26	13	30.54	5.41	MW	--	39.0	0.35
Peak slope/steady-state slope	---	8	1.04	0.02	13	1.19	0.07	t-test	19	-1.72	0.10
Initial-bursting + fast-spiking											
Max voltage change	mV	2	-70.5	---	1	-107	---	---	---	---	---
Slope of peak hyperpolarization	---	2	26.45	---	1	34.4	---	---	---	---	---
Slope of steady-state hyperpolarization	---	2	20.15	---	1	25.6	---	---	---	---	---
Peak slope/steady-state slope	---	2	1.29	---	1	1.34	---	---	---	---	---
Regular-spiking											
Max voltage change	mV	6	-105.32	14.91	12	-74.06	9.13	t-test	14	-1.90	0.08*
Slope of peak hyperpolarization	---	6	42.60	7.81	12	43.98	8.15	t-test	16	-0.11	0.92

Slope of steady-state hyperpolarization	---	6	34.62	6.69	12	37.67	7.18	MW	--	34.0	0.85
Peak slope/steady-state slope	---	6	1.24	0.11	12	1.17	0.04	MW	--	32.0	0.71
<u>Initial-bursting + regular-spiking</u>											
Max voltage change	mV	4	-69.63	10.31	4	-82.28	13.33	t-test	6	0.75	0.48
Slope of peak hyperpolarization	---	4	36.43	14.31	4	47.99	10.34	MW	--	4.00	0.25
Slope of steady-state hyperpolarization	---	4	31.18	11.62	4	43.03	10.31	t-test	6	-0.76	0.47
Peak slope/steady-state slope	---	4	1.16	0.05	4	1.13	0.03	t-test	6	0.51	0.63

[a] Properties of initial-bursting + fast-spiking cells were not analyzed statistically due to small sample sizes. N = number of cells, Stat. = test statistic, MW = Mann-Whitney U test. * = $0.10 > p > 0.05$.

Table 9. Properties of post-synaptic currents in virgin males and fathers.

		Virgins			Fathers			Analysis			
Property	Unit	N	Mean	SE	N	Mean	SE	Test	df	Stat.	P-value
Single evoked PSCs											
EPSC min	nA	15	-0.32	0.04	14	-0.25	0.02	MW	--	79.5	0.26
EPSC max	nA	15	-2.67	0.46	14	-2.17	0.31	MW	--	95.5	0.68
IPSC min	nA	22	0.33	0.04	19	0.26	0.03	t-test	39	0.13	0.14
IPSC max	nA	22	6.36	0.93	19	3.35	0.45	MW	--	111.5	0.01**
Paired-pulse ratio of ePSCs											
Inter-pulse interval											
10 ms	---	11	0.87	0.12	8	0.73	0.10	t-test	17	0.84	0.42
25 ms	---	11	0.92	0.07	8	0.89	0.18	t-test	17	0.14	0.89
50 ms	---	11	1.09	0.07	8	1.00	0.08	t-test	17	0.87	0.40
100 ms	---	11	0.92	0.07	8	0.86	0.07	t-test	17	0.58	0.57
200 ms	---	10	0.83	0.07	8	1.23	0.22	t-test	16	-1.85	0.08*
400 ms	---	10	0.88	0.08	8	0.80	0.10	t-test	16	0.65	0.53
Steady-state ratio of ePSCs											
Inter-pulse interval											
10 ms	---	11	0.49	0.08	8	0.40	0.16	MW	--	29.0	0.22
25 ms	---	11	0.61	0.06	8	0.65	0.21	MW	--	30.0	0.25
50 ms	---	11	0.89	0.17	8	0.66	0.09	t-test	17	1.09	0.29
100 ms	---	11	0.70	0.07	8	0.69	0.06	t-test	17	0.14	0.89

200 ms	---	10	0.71	0.12	8	0.92	0.17	t-test	16	-1.00	0.33
400 ms	---	10	0.57	0.09	7	0.72	0.09	t-test	15	-1.11	0.28

Paired-pulse ratio of iPSCs

Inter-pulse interval											
10 ms	---	20	0.55	0.08	14	0.35	0.05	t-test	32	1.93	0.06*
25 ms	---	20	0.77	0.05	15	0.69	0.06	MW	--	112.0	0.21
50 ms	---	20	0.87	0.05	15	0.88	0.08	t-test	33	-0.10	0.92
100 ms	---	20	0.91	0.04	15	0.92	0.10	t-test	33	-0.09	0.93
200 ms	---	20	0.89	0.04	15	0.94	0.05	t-test	33	-0.88	0.39
400 ms	---	20	0.76	0.04	15	0.84	0.08	t-test	33	-1.03	0.31

Steady-state ratio of iPSCs

Inter-pulse interval	Unit										
10 ms	---	20	0.36	0.06	15	0.31	0.07	MW	--	132	0.55
25 ms	---	20	0.63	0.06	15	0.59	0.06	t-test	33	0.42	0.68
50 ms	---	20	0.71	0.06	15	0.74	0.07	t-test	33	0.45	0.65
100 ms	---	20	0.76	0.07	15	0.79	0.08	t-test	33	-0.21	0.83
200 ms	---	20	0.74	0.04	15	0.79	0.06	t-test	33	-0.67	0.51
400 ms		20	0.72	0.04	15	0.75	0.05	t-test	34	-0.47	0.64

Spontaneous PSCs

sEPSC frequency	Hz	10	3.71	1.07	6	1.49	0.60	MW	--	14.0	0.08*
sEPSC amplitude	nA	10	-0.39	0.05	5	-0.29	0.03	t-test	13	-1.34	0.20
sIPSC frequency	Hz	21	8.46	1.94	13	6.92	1.79	t-test	32	0.54	0.59

sIPSC amplitude	nA	21	0.68	0.19	13	0.45	0.05	t-test	32	0.92	0.36

N = number of cells, PSC = post-synaptic current, EPSC = excitatory post-synaptic current, IPSC = inhibitory post-synaptic current, sEPSC = spontaneous excitatory post-synaptic current, sIPSC = spontaneous inhibitory post-synaptic current, Stat. = test statistic, MW = Mann-Whitney U test. * = $0.10 > p > 0.05$. ** = $p < 0.05$.

Table 10: Morphological properties of medial preoptic area cells in virgin males and fathers.

		Virgins (N=23 cells)		Fathers (N=22 cells)		Analysis (df=43)		
Sholl Analysis	Unit	Mean	SE	Mean	SE	Test	Stat.	P-value
Q1 (dorsal medial) intersections	#	19.17	4.47	7.86	1.76	MW	190.0	0.15
Q2 (dorsal lateral) intersections	#	13.52	3.01	14.95	2.37	MW	198.5	0.22
Q3 (ventral medial) intersections	#	10.43	2.39	15.23	3.04	MW	186.0	0.13
Q4 (ventral lateral) intersections	#	13.43	2.53	11.59	2.98	MW	232.5	0.64
Q1+Q3 (medial) intersections	#	29.61	4.47	23.09	3.52	MW	211.0	0.34
Q2+Q4 (lateral) intersections	#	26.96	4.56	26.55	4.17	MW	224.0	0.41
Medial/lateral intersections	--	1.41	0.19	2.73	1.27	MW	177.0	0.08*
Q1+Q2 (dorsal) intersections	#	32.70	5.49	22.82	2.95	MW	232.0	0.63
Q3+Q4 (ventral) intersections	#	23.87	3.60	26.82	3.82	MW	208.5	0.31
Dorsal/ventral intersections	--	1.75	0.32	1.52	0.49	MW	203.5	0.26
Total intersections	#	56.61	7.56	49.64	5.48	MW	246.5	0.88
Branch points								
Branches in Q1	#	0.96	0.28	0.45	0.13	MW	209.0	0.26
Branches in Q2	#	0.83	0.27	0.73	0.20	MW	225.0	0.48
Branches in Q3	#	0.56	0.18	0.86	0.23	MW	213.0	0.31
Branches in Q4	#	0.65	0.16	0.68	0.21	MW	235.0	0.65
Total Branches	#	3	0.43	2.64	0.51	MW	230.5	0.61
Properties of primary neurites								
Number of primary neurites	#	3.17	0.24	3.63	0.23	MW	211.0	0.33
Average length of primary neurites	µm	271.62	27.58	212.48	17.70	t-test	1.79	0.08*
Longest length of primary	µm	416.62	47.71	371.25	30.82	t-test	0.79	0.43

neurites								
Total length of primary neurites	µm	903.42	123.49	793.47	86.65	MW	244.0	0.84
Properties of secondary neurites								
Number of secondary neurites	#	2.78	0.39	2.09	0.31	MW	218.5	0.43
Average length of secondary neurites	µm	102.37	19.91	97.88	12.91	MW	223.0	0.50
Longest length of secondary neurites	µm	172.95	29.89	153.94	26.66	MW	245.0	0.86
Total length of secondary neurites	µm	359.31	72.89	253.46	53.34	MW	238.0	0.73
Properties of tertiary neurites								
Number of tertiary neurites	#	0.39	0.14	0.32	0.17	MW	220.5	0.33
Average length of tertiary neurites	µm	28.38	11.60	6.22	3.01	MW	207.5	0.17
Longest length of tertiary neurites	µm	28.69	11.66	7.45	3.92	MW	207.5	0.17
Total length of tertiary neurites	µm	35.35	13.80	12.30	7.24	MW	210.5	0.20
Other morphological properties								
Total neurite length	µm	1296.4	178.02	1055.69	123.99	MW	244.0	0.84
Largest soma diameter	µm	18.81	1.48	17.73	0.65	MW	250.0	0.95
Soma circumference	µm	55.41	4.03	54.06	2.40	MW	246.0	0.87

Q = quadrant, Stat. = test statistic, MW = Mann-Whitney U test. * = $0.10 > p > 0.05$.

Supplemental Table 1. Correlations of selected behavioral and neuronal measures in virgin males.

	Latency to engage in paternal care			Percent time in paternal care		
	r_s	P-value	N	r_s	P-value	N
Input resistance in K-based solution	-0.09	0.78	15	0.11	0.69	15
Threshold to AP	-0.01	0.98	14	0.08	0.79	14
AP amplitude	-0.68	0.007*	14	-0.17	0.57	14
AP half-width	0.34	0.23	14	0.35	0.23	14
fAHP at 3-5 msec	0.38	0.18	14	0.04	0.9	14
Maximum number of APs	0.02	0.96	13	0.15	0.62	13
Minimum average AP ISI	0.09	0.76	13	-0.12	0.71	13
Minimum average AP ISI	0.06	0.84	13	0.41	0.17	13
Tau from ISI exponential fit	0.13	0.68	13	0.04	0.91	13
mAHP	-0.01	0.96	13	-0.14	0.69	13
sAHP	0.25	0.41	13	0.23	0.47	13
Maximum voltage change in response to hyperpolarizing current	0.67	0.009*	14	-0.12	0.67	14
Input resistance in Cs-based solution	-0.48	0.23	8	0.48	0.23	8
EPSC min	0.49	0.22	8	-0.54	0.17	8
EPSC max	-0.14	0.75	8	0.50	0.21	8
IPSC min	-0.67	0.07	8	-0.15	0.72	8
IPSC max	-0.27	0.52	8	-0.25	0.56	8
sEPSC frequency	-0.30	0.51	7	0.40	0.37	7
sEPSC amplitude	-0.28	0.54	7	0.05	0.92	7
sIPSC frequency	-0.07	0.86	8	0.29	0.49	8
sIPSC amplitude	0.16	0.70	8	-0.08	0.87	8
Total Sholl intersection	-0.01	0.98	7	0.03	0.95	7
Total branches	0.40	0.37	7	-0.22	0.64	7
Total neurite length	-0.27	0.60	6	0.21	0.69	6

Largest soma diameter	-0.95	0.001*	7	0.84	0.17	7

Spearman correlations between key infant-directed behaviors and neuronal properties in virgin males. After correcting for false discovery rate, none of the correlations were statistically significant. * = nominal significance, $p < 0.05$. N = number of cells, AP = action potential, ISI = inter-spike interval, fAHP = fast afterhyperpolarization, mAHP = medium afterhyperpolarization, sAHP = slow afterhyperpolarization, PSC = post-synaptic current, EPSC = excitatory post-synaptic current, IPSC = inhibitory post-synaptic current, sEPSC = spontaneous excitatory post-synaptic current, sIPSC = spontaneous inhibitory post-synaptic current. See methods for full description of metrics.